

University of Louisville

ThinkIR: The University of Louisville's Institutional Repository

Electronic Theses and Dissertations

12-2023

Genetically engineering Gingipains for high yield large scale purification.

Andrew E. Fuchs
University of Louisville

Follow this and additional works at: <https://ir.library.louisville.edu/etd>



Part of the [Oral Biology and Oral Pathology Commons](#)

Recommended Citation

Fuchs, Andrew E., "Genetically engineering Gingipains for high yield large scale purification." (2023).
Electronic Theses and Dissertations. Paper 4193.
<https://doi.org/10.18297/etd/4193>

This Master's Thesis is brought to you for free and open access by ThinkIR: The University of Louisville's Institutional Repository. It has been accepted for inclusion in Electronic Theses and Dissertations by an authorized administrator of ThinkIR: The University of Louisville's Institutional Repository. This title appears here courtesy of the author, who has retained all other copyrights. For more information, please contact thinkir@louisville.edu.

GENETICALLY ENGINEERING GINGIPAINS FOR HIGH YIELD LARGE SCALE
PURIFICATION

By

Andrew E. Fuchs

B.S., University of Louisville, 2015

A Thesis

Submitted to the Faculty of the School of Dentistry of the University of Louisville

In Partial Fulfillment of the Requirements

For the Degree of

Master of Science

in Oral Biology

Department of Oral Immunology and Infectious Diseases

University of Louisville

Louisville, Ky

December 2023

GENETICALLY ENGINEERING GINGIPAINS FOR HIGH YIELD LARGE SCALE
PURIFICATION

By

Andrew E. Fuchs

B.S., University of Louisville, 2015

A Thesis approved on

August 31, 2023

by the following Thesis Committee:

Dr. Jan Potempa, Thesis Director

Dr. Juhi Bagaitkar

Dr. James Graham

Dr. Silvia Uriarte

DEDICATION

To my son, Benjamin, who has been more accommodating than I could ever possibly expect a 16-month-old to be when told Daddy had to work on this thesis at night instead of playing.

ACKNOWLEDGEMENTS

Thanks to my committee members, Juhi Bagaitkar, James Graham, and Silvia Uriarte, for their time and guidance. To Michele Pisano, who went out of her way to admit me to the program, and to structure the course work to my unique situation. To Jan Potempa, who took a chance on a technician with little skills or experience and is always happily willing to sacrifice his valuable time to teach others.

Special thanks to Barbara Potempa, who has constantly challenged me to better myself, and pushed me to begin this journey. She has been a steadfast champion for me, and without her influence I would not be writing this today. I am eternally grateful for her support.

Finally, to my wife Emily, who has been a source of unwavering support through this process, even while we welcomed our son Benjamin into our family. She has shouldered a truly unfair amount of the domestic burden of new parenthood while also working herself. I am in awe of her and consider myself truly fortunate to know her.

ABSTRACT
GENETICALLY ENGINEERING GINGIPAINS FOR HIGH YIELD LARGE SCALE
PURIFICATION

Andrew E. Fuchs

8/31/23

Porphyromonas gingivalis is a keystone oral pathogen in the progression of periodontal disease and has been implicated in the etiology of many other systemic human diseases. *P. gingivalis* produces primary virulence factors termed the gingipains, a group of cysteine proteases. There is a high demand for high purity gingipains for downstream *in vitro* studies where *P.g.* is implicated, both oral and systemic. Gingipain production candidate mutant *P.g.* strains were generated to isolate each gingipain for large scale purification and the purified gingipains characterized. Two mutants were determined not to be viable for large scale purification of gingipains, each for different reasons, which may give some insight into novel mechanisms of adaption in *P. gingivalis*.

TABLE OF CONTENTS

DEDICATION.....	iii
ACKNOWLEDGEMENTS	iv
ABSTRACT.....	v
LIST OF FIGURES	vii
INTRODUCTION.....	1
GINGIPAINS.....	5
PROTEIN PURIFICATION	9
PREVIOUS WORK	11
NEW STRAINS.....	14
GOALS.....	17
RESULTS.....	18
W83 Δ WbpB Kgp8HSLA (Kgp8H).....	18
W83 Δ Kgp RgpB8HTSI (RgpB8H)	26
W83 Δ WbpB RgpA-YIP6HIS (RgpA6H).....	29
DISCUSSION.....	33
FUTURE WORK	38
MATERIALS AND METHODS.....	40
REFERENCES.....	50
CURRICULUM VITA	53

LIST OF FIGURES

1. Hypothetical model of T9SS cargo protein secretion.....	3
2. Domain scheme of gingipain zymogens.	7
3. Scheme for catalytic processing of gingipain zymogens	8
4. KgpP1 mutant	11
5. RgpB6H mutant	13
6. Kgp8H mutation scheme	15
7. RgpA6H mutation scheme	15
8. RgpB8H mutation scheme	16
9. Kgp8H Nickel-Sepharose Elution Fraction data.....	19
10. Kgp8H prep 1 characterization data.....	20
11. Kgp8H prep 1 activity recovery.....	21
12. Kgp8H prep 4 characterization data.....	22
13. Kgp8H small scale characterization data	24
14. RgpB8H prep 1 characterization data	26
15. RgpB8H small scale activity recovery.	28
16. RgpB8H profragment degradation	28
17. RgpA6H prep 1 characterization data	30
18. RgpA6H small scale characterization data	32

INTRODUCTION

In 2021, the World Health Assembly voted to include oral health in the non-communicable disease category, and further recommended that oral health treatment and prevention should be included in universal healthcare programs, highlighting the importance of oral health to overall systemic health. About 1 billion cases of severe periodontal disease were reported worldwide in 2019. When combined with other aspects of oral health, untreated caries and edentulism, total oral health cases were larger than the next 5 most prevalent non-communicable diseases, combined⁶. This list includes cardiovascular disease, diabetes mellitus, cancers, and chronic respiratory diseases. Chronic periodontal disease, or periodontitis, is a major factor of overall oral health, but also has been implicated in many other systemic diseases, such as diabetes mellitus, respiratory disease, cardiovascular disease, osteoporosis⁷, preterm birth⁸, low birth weight^{9, 10}, metabolic syndrome¹¹, rheumatoid arthritis¹², atherosclerosis¹³, cancer¹⁴, and Alzheimer's disease¹⁵. This highlights the importance and relevance of oral health to the overall health and well-being of the individual.

Periodontitis is characterized as a chronic inflammatory disease driven by bacterial colonization of the tooth surface below the gum line¹⁶. However, unlike

an acute infection, where an invading pathogen at a site of injury can be challenged and eventually cleared by the host immune response, the oral cavity is host to many species of beneficial commensal bacteria, which the host immune response naturally tolerates¹⁷. When healthy, the host immune response and the bacterial microbiota maintain a homeostatic state. Periodontitis occurs when the homeostasis is disrupted and composition of the oral microbial community shifts from a predominantly commensal makeup to a dysbiotic community that includes periodontopathogens, with *Porphyromonas gingivalis*, *Treponema denticola*, and *Tannerella Forsythia* being strongly associated with the disease¹⁸. Of these, *P. gingivalis* has been termed a keystone pathogen in the etiology of periodontitis, due to its relatively small abundance in dysbiotic biofilms but with disproportionately large effects on its microbial community and host tissues¹⁹.

P. gingivalis is one of the more well studied members of the periodontopathogens, due to its status as a keystone pathogen in periodontitis, as well as its relative ease of culturing compared to the other known pathogenic species. *P. gingivalis* is a gram-negative obligate anaerobe bacterium that produces many virulence factors to influence its environment. As a gram-negative bacterium, *P. gingivalis* has both an inner and outer membrane, which must be transited to successfully secrete proteinaceous virulence factors that are produced in the cytoplasm. *P. gingivalis* uses the sec transporter system to move cargo proteins across the inner membrane (IM) to the periplasm, then uses the type IX secretion system (T9SS) to export the cargo across the outer membrane

(OM)¹ (Figure 1). With a two-step transport system different methods are required to properly identify cargo proteins for transport, which come in the form of an N-terminal sec signal sequence²⁰ for the IM sec system, and a C-terminal domain (CTD) sequence for transport by the OM T9SS²¹.

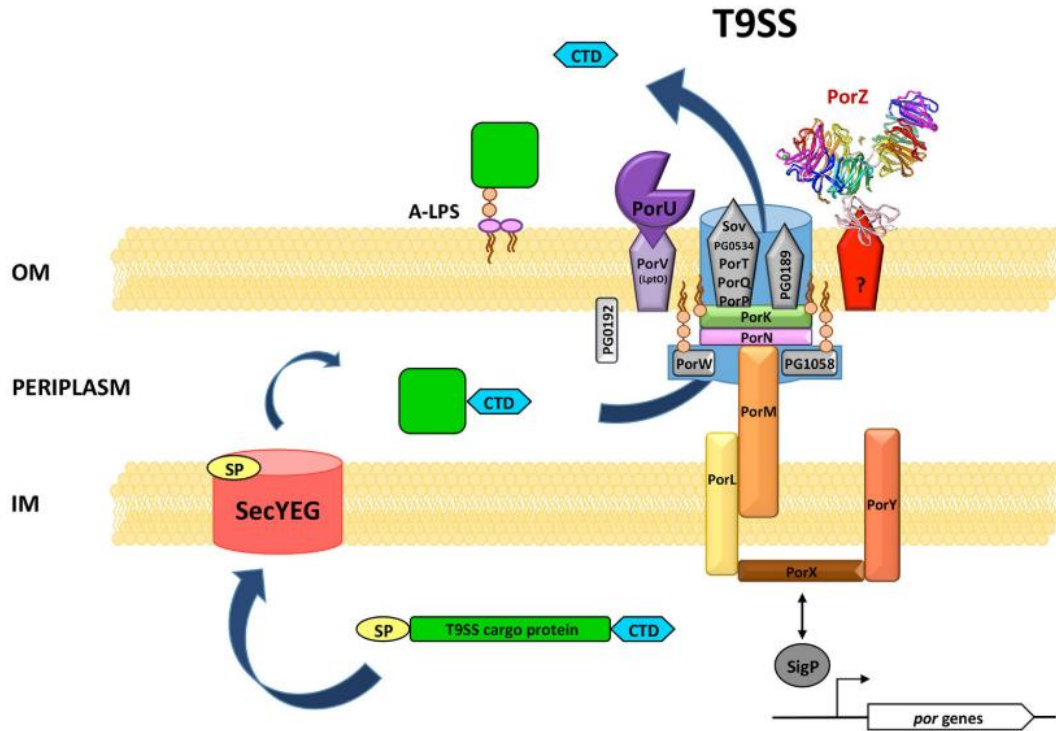


Figure 1 – Hypothetical model of Type 9 secretion system. Overall structure not currently known and displayed as a blue background with known components. Cargo proteins are translocated across the Inner Membrane by the Sec system via the N-terminal signal peptide. Cargo protein folding occurs in the periplasm. C-terminal domain signals for translocation through the T9SS. PorU functions in a sortase-like manner, removing the CTD from the cargo protein and attaching the cargo to the outer membrane by glycosylation with anionic LPS. Adapted¹

As the only currently identified protein secretion system for *P. gingivalis*¹, understanding the mechanism of secretion for the T9SS has been a tempting target for investigation. Studies on the CTD have shown that exact sequence specificity is not required for transport; rather that the structure of the CTD is key for T9SS transport²². Modifications to the structural motifs of the CTD can either cause cargo to be stuck in the periplasm²² or prevent the glycosylation and

attachment of the cargo to the OM with anionic lipopolysaccharides(A-LPS), causing the cargo protein to be secreted into the extracellular space²³. A wild-type *P. gingivalis* strain, HG66, has demonstrated this particular secretory behavior, and was discovered to have a LOF mutation in the *wbpB* gene responsible for the production of A-LPS, and subsequently the successful surface attachment of T9SS cargo proteins²⁴.

GINGIPAINS

Cargo for the T9SS includes the gingipains, a family of cysteine proteases that account for up to 85% of the total proteolytic activity associated with the bacterium²⁵. These trypsin-like proteases are one of the major virulence factors of *P. gingivalis* and are critical to the survival and host immune modulation abilities of the bacterium. Gingipains have been shown to be critical for evading host immune response²⁶, heme acquisition²⁷, host tissue penetration^{28, 29}, degradation of complement proteins³⁰, activation of blood coagulation, platelet aggregation, cytokine degradation, and enhance expression of matrix metalloproteinases³¹. This widespread effector ability is in part due to the relatively broad range of proteolytic activity available to the gingipains.

There are two members of the gingipains with specificity for arginine (Arg) at the P1 position, R gingipain A (RgpA) and R gingipain B (RgpB)². They are highly specific proteases for Arg at the P1 position but will hydrolyze bonds with any amino acid at the P1' position, giving endopeptidase activity at any Arg-Xaa bond. They have also been shown to exhibit limited carboxypeptidase and aminopeptidase activity with n-terminal and c-terminal Arg substrate residues, respectively³².

The last member of the gingipains is K gingipain (Kgp), with specificity for lysine (Lys) at the P1 position. Like the R gingipains, it is also highly specific for the P1 position and accepts any residue at P1' for endopeptidase activity at any Lys-Xaa bond, however some residues in the P2 position (Arg,Lys) makes a Lys-Xaa peptide bond in the sequential motif Lys/Arg-Lys-Xaa resistant to proteolytic cleavage by Kgp⁵.

Structurally, gingipains are composed of several shared motifs (Figure 2). All gingipains have an N-terminal sec signal for transportation across the IM sec system, followed by a profragment and catalytic domain. The profragment functions as an inhibitor for the catalytic domain during transport and maturation of the zymogen, until transport through the T9SS, where it is eventually cleaved and cleared³³. In RgpA and Kgp, the catalytic domain is followed by an immunoglobulin-like domain and a series of hemagglutinin/adhesin domains, HA1-4. Finally, all three gingipains have the C-terminal domain motifs necessary for secretion by the T9SS^{2,5}. The catalytic domain for RgpA and RgpB are highly homologous, with most variances occurring in the C-terminal region, away from the catalytic center³⁴, which shares a 97% identity among the caspase-like folds³⁵. After maturation and secretion through the T9SS, the HA domains have been cleaved and form a non-covalent complex together with the catalytic domain (Figure 3). The CTD signal is cleaved off during A-LPS attachment, leaving the whole complex anchored into the membrane. In *P. gingivalis* strains that have deficiencies in the A-LPS synthesis pathway, the CTD region is still

removed from the enzyme, but without A-LPS available as a membrane attachment point the protein is secreted into the surrounding media.

Gingipains are considered one of the primary virulence factors of *P. gingivalis* due to unrestrained proteolytic activity against a broad array of host

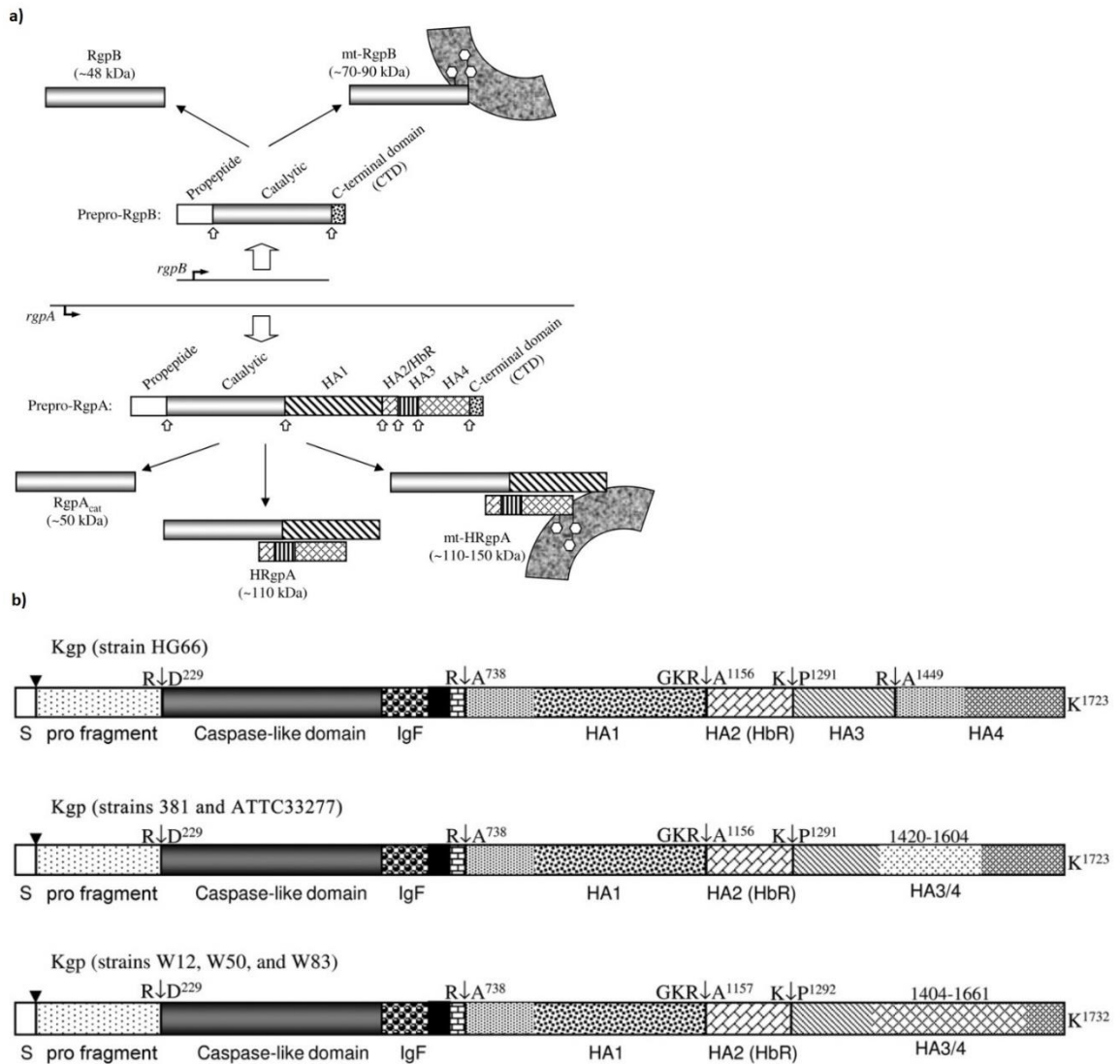


Figure 2 - a) Domain scheme for zymogens produced by *RgpB* and *RgpA* genes. Cleavage sites for maturation denoted by arrows. Adapted² **b)** Domain scheme for *Kgp* zymogen from multiple strains, highlighting variability in HA domain processing. Adapted⁵

proteins, the essential role in the acquisition of nutrients, and participation in the maturation of other virulence factors^{36, 37}. Mutant strains deficient in gingipain activity are not pathogenic in various animal models of infection^{36, 38, 39}. To further investigate the role gingipains play in various in vitro and in vivo models, as well as solve the crystal structure via x-ray crystallography, they first must be isolated and purified.

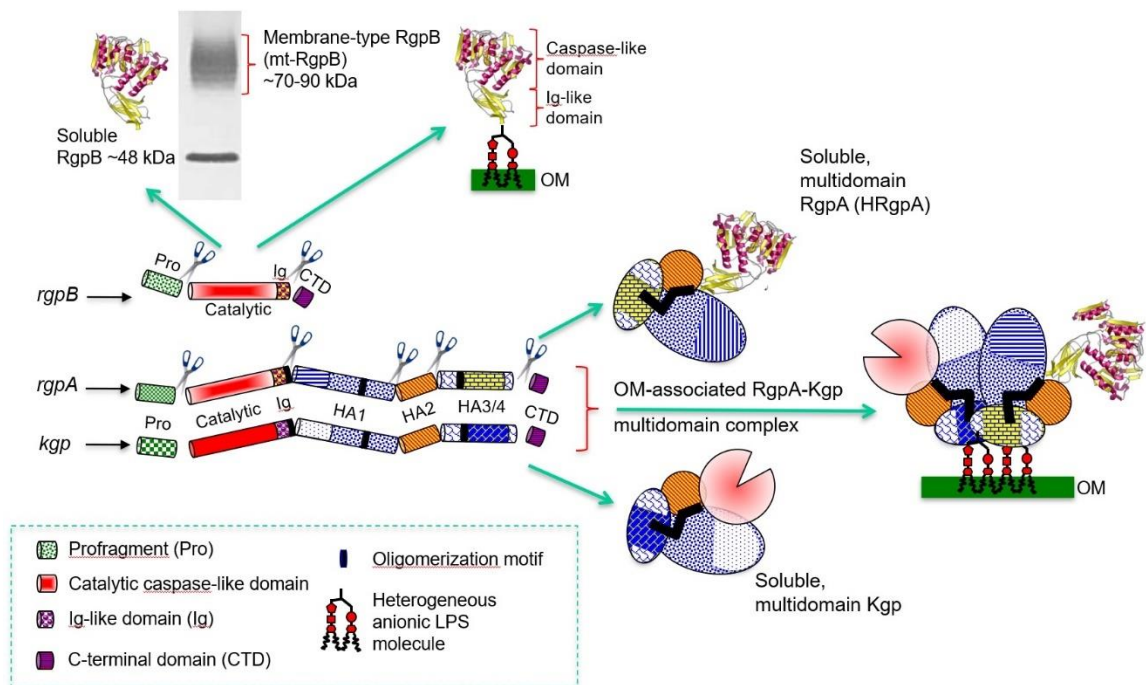


Figure 3- Scheme for catalytic processing of gingipain zymogens. Gingipain domains are cleaved then either attached to the outer membrane by glycosylation with OM-associated A-LPS or secreted in a soluble form. RgpA and Kgp are assembled into non-covalent multidomain complexes consisting of their catalytic domains and hemagglutinin/adhesin domains. RgpA and Kgp complexes also form non-covalent associations with each other. Adapted³

PROTEIN PURIFICATION

Purification of membrane-bound proteins is possible with membrane disruption and the use of detergents but will leave the purified proteins with heterologous saccharide residues at the membrane attachment point, which is not acceptable from a crystallography standpoint⁴⁰. Further, the steps necessary for membrane processing are laborious and not ideal for large-scale purification. A common method of producing proteins suitable for X-ray diffraction analysis is to produce the recombinant protein in *Escherichia coli*, using commercially available and widely used plasmid expression systems. However, this is not viable for gingipains due to their proteolytic activity, as well as the maturation process in *P. gingivalis* being required for proper folding. When the expression of gingipains is activated, the cytotoxic effects rapidly kill the host *E. coli* and halt further gingipain production. Due to the role the T9SS plays in the proper maturation of gingipains, there is an open question of whether any gingipains produced in other species without a T9SS would be properly analogous to wild-type enzymes. For these reasons it is necessary to produce modified gingipains in *P. gingivalis* strains.

The discovery of wild-type strain HG66 and its secretion of gingipains into the extracellular environment was a key step in the initial purification of

gingipains⁴¹. By using a strain that secreted the target protein into the extracellular space, any membrane manipulation could be avoided, and the proteins could be precipitated and purified solely from the cell culture media. By using the differing affinities of each enzyme, Kgp and RgpA/B could be separated by affinity chromatography, then RgpA/B further separated by size exclusion chromatography, due to RgpA being complexed with HA domains and having a larger molecular mass. This worked well; however, the affinity separation was never perfect and some low level of gingipain cross-contamination always persisted. Investigation into HG66 revealed the WbpB mutation that caused this secretion behavior²⁴, which could be used for future mutant strains.

To strengthen the affinity separation, a common technique used is the addition of an affinity tag into the gene of the protein of interest⁴². A six-histidine repeat is commonly used as an affinity tag to readily bind onto a nickel-Sepharose matrix, where it can be washed then eluted in a purified form. This strategy has been used in previous *P. gingivalis* mutants for RgpB and Kgp.

PREVIOUS WORK

A six-histidine tag insertion was previously used to investigate the oligomerization motif in the catalytic domain of Kgp⁴ (Figure 4). Disruption of the oligomerization motif would prevent formation of the non-covalent complex of the catalytic domain with the hemagglutinin/adhesin domains. A series of mutations, both inserts and overwrites, were designed to disrupt the oligomerization motif. The CTD signal was present at the end of the polypeptide after the HA domains and serves as the site of attachment to the OM. By preventing the catalytic domain from complexing with the membrane bound HA domains, the catalytic domain was secreted into the surrounding media. This provided a mutant producing

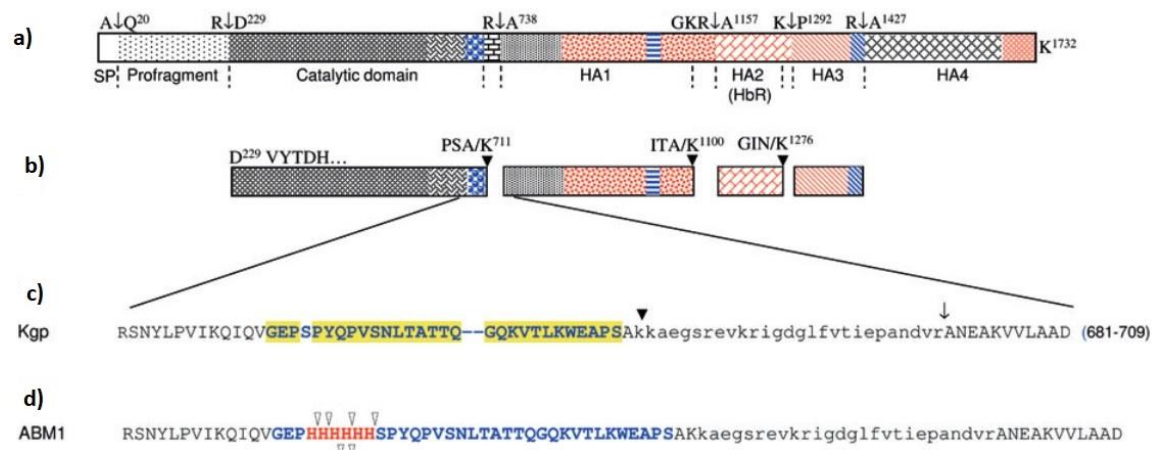


Figure 4 a) full domain scheme of W83 Kgp pre-processing. b) Remaining domains of Kgp after maturation and processing. c) Amino acid sequence from the C-terminal region of the Kgp catalytic domain. Blue color indicates adhesin binding (oligomerization) motif. Yellow highlight indicates homologous residues with sequence of RgpA. d) the 6-His insertion into the oligomerization motif that generated the KgpP1 mutant to produce soluble Kgp catalytic domain. Adapted⁴.

soluble His-tagged Kgp catalytic domains (Kgp_{cat}), however it came with several drawbacks. The total Kgp activity produced was only one third that of the wild type, and this reduction was confirmed to not be expression based, so was theorized to be a product of misfolded proteins, likely during the maturation process. The soluble activity that was present was subjected to affinity chromatography and was found to have only 6-7% intact six-His tags, based on Kgp activity. Investigation of the affinity flowthrough found peptides with mono-, di-, and tetra-histidine repeats, indicating truncation of the his-tag had led to the low affinity binding. Nevertheless, this mutant remained a good source of Kgp catalytic domain for further downstream in vitro and in vivo studies for several years, before eventually >99% of Kgp activity exhibited this same truncation of the His-tag.

For RgpB, a mutant termed RgpB6H had been generated in W83 background that took advantage of the structure of the CTD to cause secretion into the external media²³ (Figure 5). By adding a six histidine repeat tag at a specific point N-terminal to the CTD, the structural conformation was changed sufficiently to prevent attachment of A-LPS to the enzyme. This mutant was highly successful at producing the gingipain RgpB, which consists of the catalytic domain of the arginine gingipains and an Ig-like fold. Purification of RgpB allowed for investigation into the effects of arginine proteolytic activity in various in vitro and in vivo models. While strains with such a mutation should only secrete RgpB into the extracellular space, RgpB purified from this mutant always exhibited low levels of lysine-specific proteolytic activity, indicating some level of contamination

with Kgp catalytic domains. Further purification by affinity chromatography could not separate these activities and similarities in pI, molecular mass and other physicochemical properties make the use of other chromatographic approaches such as size exclusion, ion exchange, and hydrophobic interactions not appropriate.

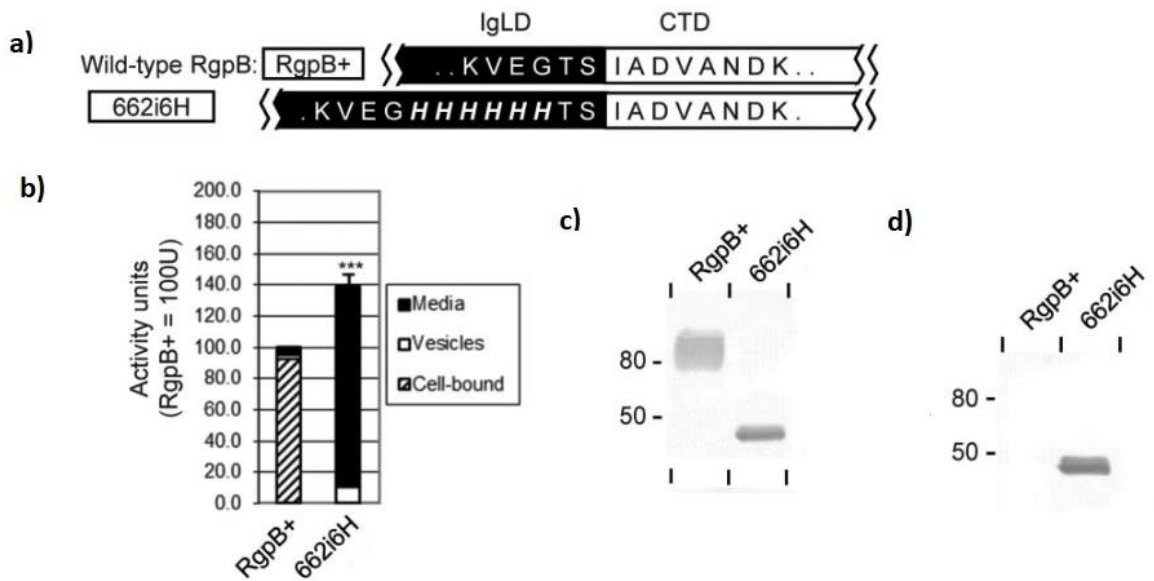


Figure 5 – construction of RgpB6H mutant (662i6H) a) insertion of 6xHis tag into RgpB gene b) localization of Rgp in RgpB6H mutant is predominantly in media compared to the prevalent cell-bound association found in wild type c) Western blot for anti-RgpB shows sharp secretion band at ~47kDa for RgpB6H compared to the diffuse membrane-associated RgpB found in wild type d) western blot against anti-6xHis shows successful expression of His-tag in RgpB6H. Adapted^{d22}

NEW STRAINS

Three new strains were generated, one for each gingipain, to address different goals for each enzyme. Kgp had previously been purified in its catalytic domain form from the KgpP1 strain; however, this strain eventually showed the same affinity tag truncation seen in other candidates during the mutant construction. To address this truncation, a new mutant was devised with an insertion of eight histidine repeats. KgpP1 had been successful at producing a catalytic domain pure enough for X-ray crystallography to solve the structure, but the structure of the full-length Kgp protein remains unsolved. This new mutant was designed to produce full-length Kgp protein with an affinity tag in sufficient purity and quantity to be viable for X-ray crystallography analysis. Rather than achieve protein secretion through disruption of the CTD structure with the His-tag insertion, this mutation was made in a W83 background strain with a deletion in the WbpB gene, a key factor in the generation of A-LPS. This allowed for screening several potential insertion points for the affinity tag. The mutant candidate selected for this project had an eight-histidine insertion n-terminal to the SLA amino acid sequence in the Kgp gene (Figure 6). The name for this mutant is W83 Δ wbpB Kgp8HSLA, or Kgp8H.

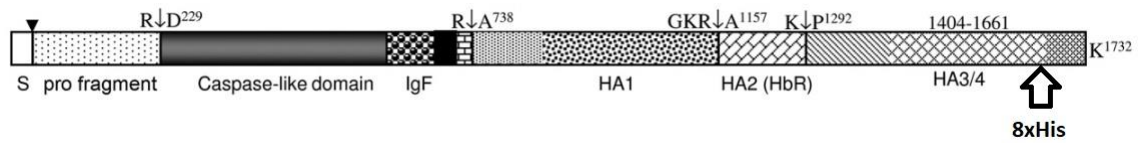


Figure 6- Domain scheme for Kgp8H prepro-peptide with arrow indicating mutation for affinity tag insertion.

RgpA had similar design goals to Kgp; a full-length RgpA affinity mutant has not been successful to date. A six-histidine affinity tag insertion was planned into the RgpA gene to produce soluble full-length RgpA that would be suitable for characterization and X-ray crystallography. The mutant was also made in the W83 Δ wbpB background to allow for secretion of all T9SS carrier proteins and allow for a larger range of potential 6-His tag insertion targets. The candidate

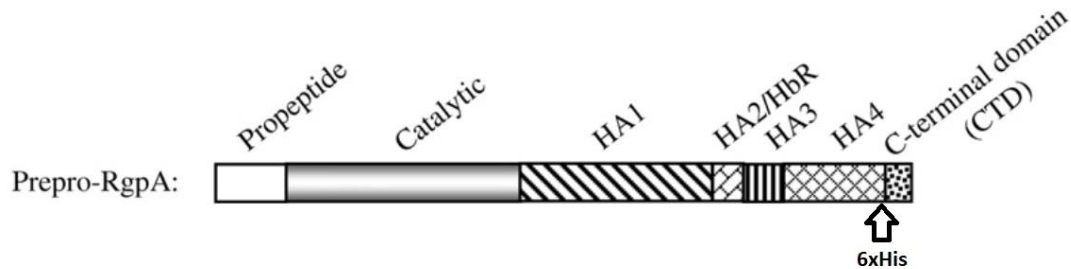


Figure 7 – Domain scheme for RgpA6H prepro-peptide with arrow indicating location of affinity tag insertion.

mutant selected for this project had the 6-His insertion made c-terminal to the YIP sequence of the final HA domain, just before the beginning of the CTD (Figure 7). This allowed for processing by the T9SS and secretion of full-length RgpA. This mutant was termed W83 Δ wbpB RgpA-YIP6HIS, or RgpA6H.

RgpB had been successfully purified from the strain RgpB6H in the past, however enzymes purified from this strain always had low levels of Kgp lysine specific proteolytic activity present. To produce purified RgpB without this trace contamination, a new mutant was planned in a Δ Kgp background. This mutant

was also designed with an 8-His tag to prevent any potential truncation seen in previous 6-His Kgp strains. The mutation was made N-terminal to the TSAID

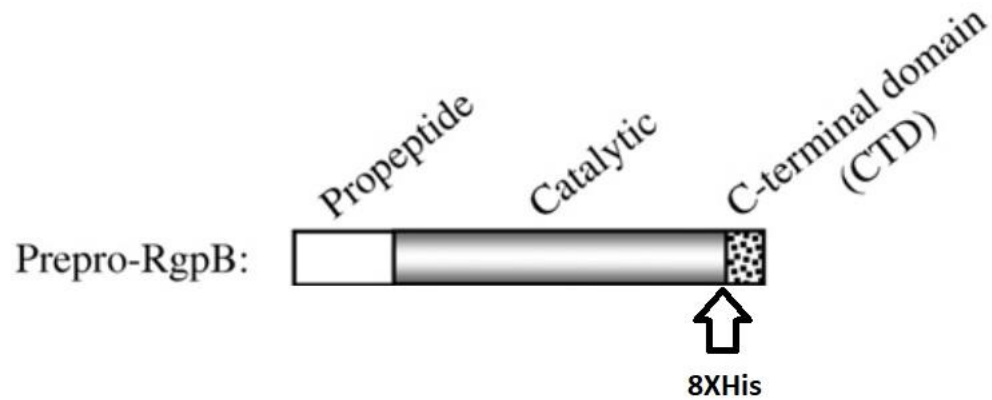


Figure 8 – Domain scheme for RgpB8H prepro-peptide with arrow indicating location of affinity His tag insertion.

sequence in the RgpB gene, which is the same insertion point (662) used in the previous RgpB6H mutant. This insertion point disrupts the proper attachment of the enzyme to A-LPS after removal of the CTD, causing the secretion of RgpB (Figure 8). This mutant was termed W83 Δ Kgp RgpB8HTSI, or RgpB8H.

GOALS

This project initially started with the goal of performing large scale purifications of each mutant to determine the viability of each mutant to produce targeted gingipains and determine the yield and scalability of those gingipains. These gingipains would then be characterized to determine their proteolytic and biochemical properties. As the project progressed, a new goal of gaining insights into the unknown processes of gingipain maturation and profragment degradation was also added.

RESULTS

W83 Δ WBPB KGP8HSLA (KGP8H)

Mutant Kgp8H was generated by insertion of an 8-His repeat N-terminal to the SLA pattern of the CTD. The SLA motif is the first residues of the CTD and should be removed from the final gingipain by the normal maturation process. This leaves the His tag attached to the C-terminal HA domain after maturation and allows for the affinity purification of the full non-covalent complex. In total, eight large-scale purifications and three small-scale were performed. The first large scale purification was 10 liters and was performed according to protein purification method. After nickel-Sepharose affinity chromatography, fractions were collected from elution and assayed for Kgp activity (Figure 9). Two fractions exhibiting the highest activity were sampled for western blot analysis and N-terminal sequencing of the detected HA domains (Figure 10). Western blot for the recurring YTYTVYRDG motif in the HA domains showed unexpected processing, with five distinct band patterns for only two motif repeats in the Kgp gene. Blotting for anti-6xHis showed two low molecular weight bands as well as a band around 50 kDa, indicating aberrant processing of the HA4 domain. N-terminal sequences showed proper processing of catalytic and HA1 domains; however, no sequences for HA2/3 were detected. Several unusual cleavage sites were

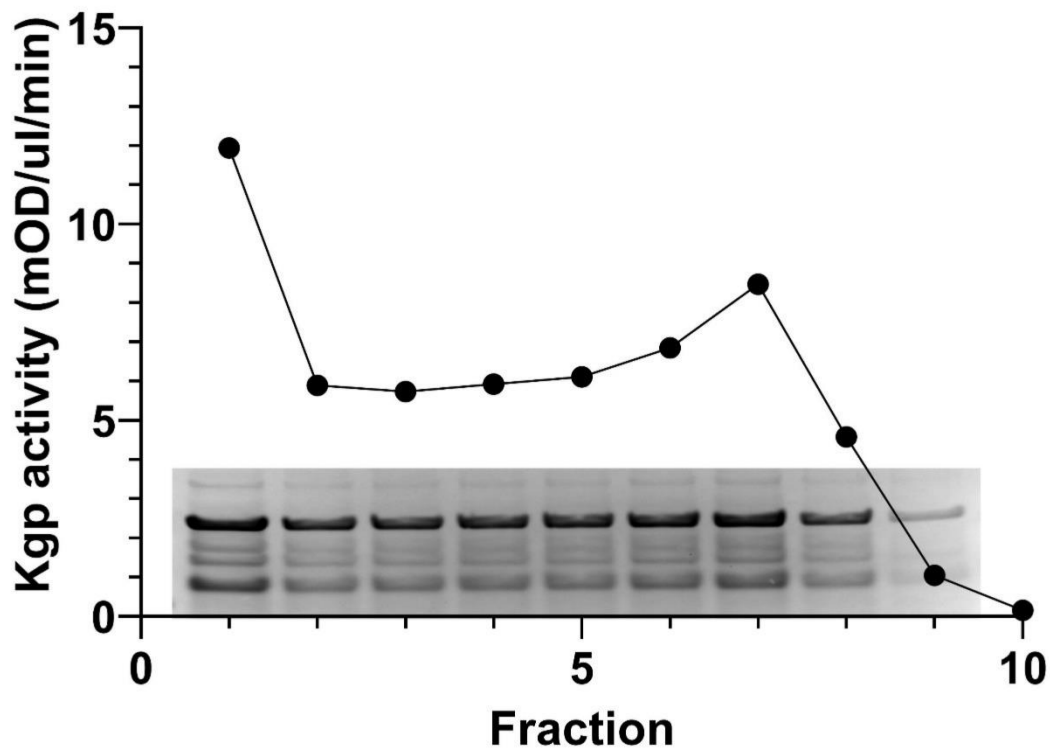


Figure 9- Graph of Kgp activity in each fraction of nickel-Sepharose elution. SDS-page analysis of each fraction is overlaid, indicating fraction homogeneity.

found in the HA4 domain, including at methionine and threonine residues, indicating proteolytic activity not commonly seen in *P. gingivalis*. The affinity purification was serviceable, with a total Kgp activity recovery of 3.1% compared to the initial cell culture activity (Figure 11).

The following two large scale purifications (Prep 2+3) were 20 liters, but both lost Kgp activity at the 20L culture stage. At the time it was considered an anomaly with the anaerobic chamber environment, growth conditions, or potential contamination, but Rgp activity in the 20L culture remained consistent through all three purifications at the culture stage.

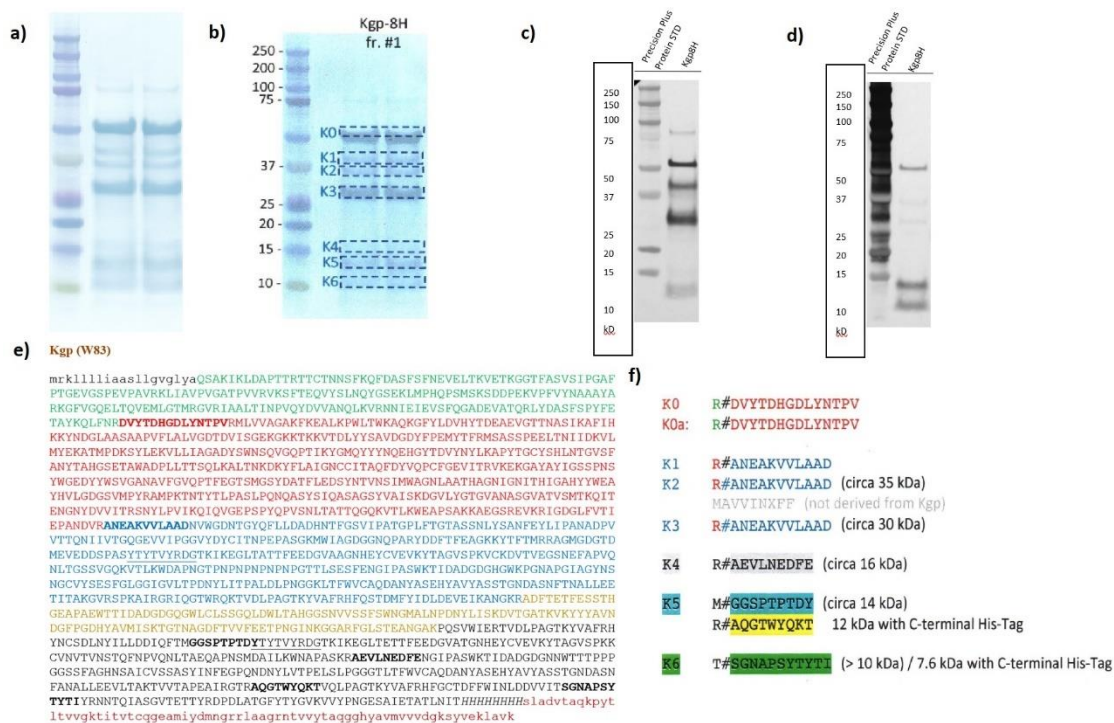


Figure 10– N-terminal sequencing of Kgp8H purification product a) Protein transfer to PVDF membrane visualized with comassie blue for N-terminal sequencing. Two elution samples exhibited the same banding patterns. b) Seven distinct bands were identified for N-terminal sequencing. c) Western blot for anti-YTYTVYRDG (Anti-HA), a recurring motif in the HA domains revealed 5 distinct bands. d) Western blot for anti-6xHis tag showed two low molecular weight bands and one band at 50 kDa. e) Amino acid sequence for the Kgp gene in mutant Kgp8H. Canonical domain structures are separated by color. N-terminal sequence cleavage sites are denoted in bold. Recurring YTYTVYRDG motif for anti-HA antibodies is underlined. f) N-terminal residue sequences for identified bands. Cleavage site denoted with #.

Prep 4 was the first successful 20L prep of the large-scale purifications, with nearly 32% of the total Kgp activity recovered in the nickel-Sepharose eluate. Analysis of western blot confirmed the presence of the Kgp catalytic domain, HA domains, and His tag, indicating successful purification of full length Kgp (Figure 12). The banding patterns were similar to those found in purification 1, with minor changes in relative band intensities. The final yield of the purified enzyme was 6.13 mg, or 0.307 mg/L of culture.

The remaining large-scale preps, 5-8, all had similar issues arise. The first issue was the presence of a white precipitate in the acetone pellet after resuspension in ion exchange buffer. At this stage of the purification process, the

Kgp8H Prep 1 10L Kgp activity %

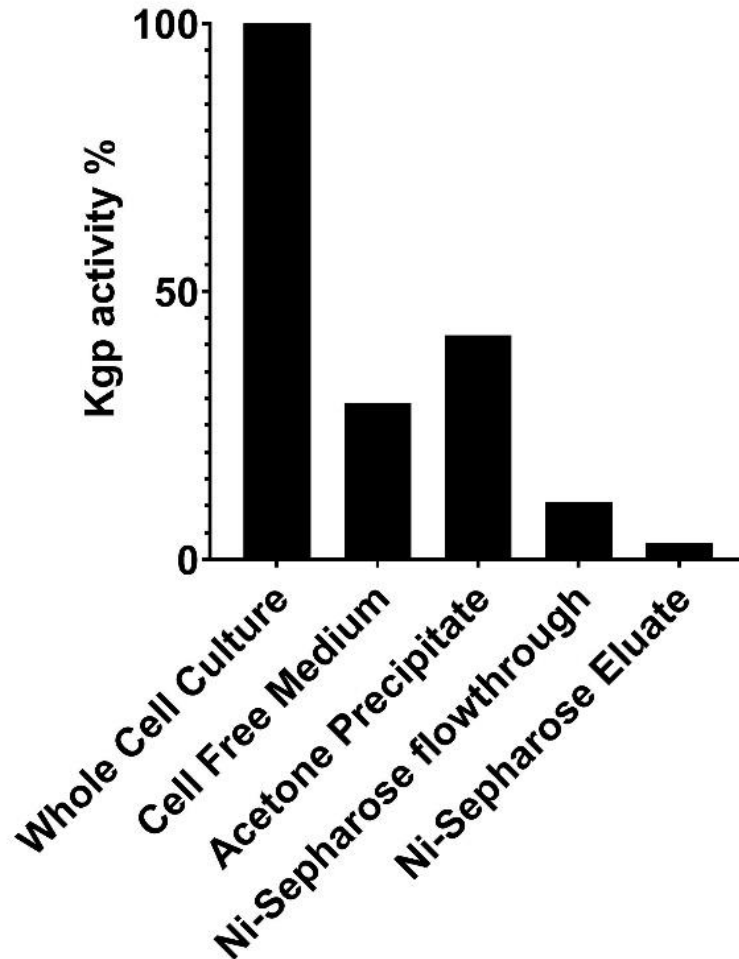


Figure 11- Retained Kgp activity expressed as a percent of initial whole cell culture activity (WCC) at each subsequent purification step for large scale purification 1.

proteins have been collected from the media by acetone precipitation and should readily resolubilize after dialysis. In these purifications, however, the presence of this insoluble white precipitate accompanied a drop in Kgp activity. This was first detected after centrifuging the dialyzed acetone pellet to remove insoluble materials; Rgp activity loss was around 6% while Kgp activity loss was 46%.

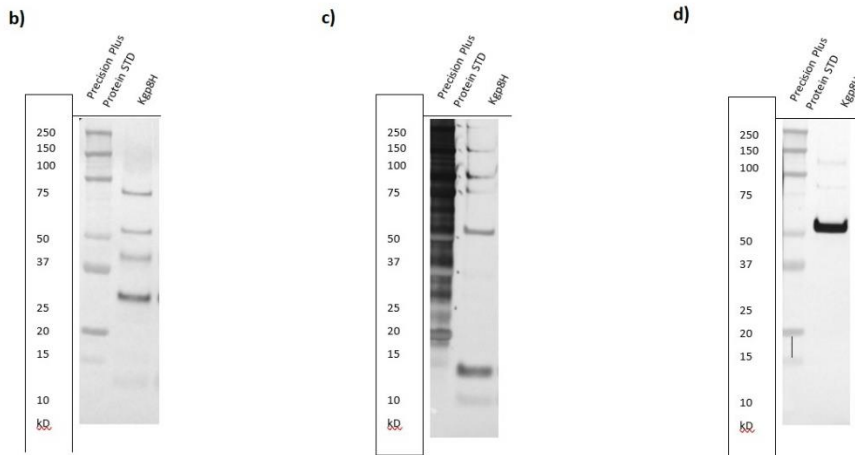
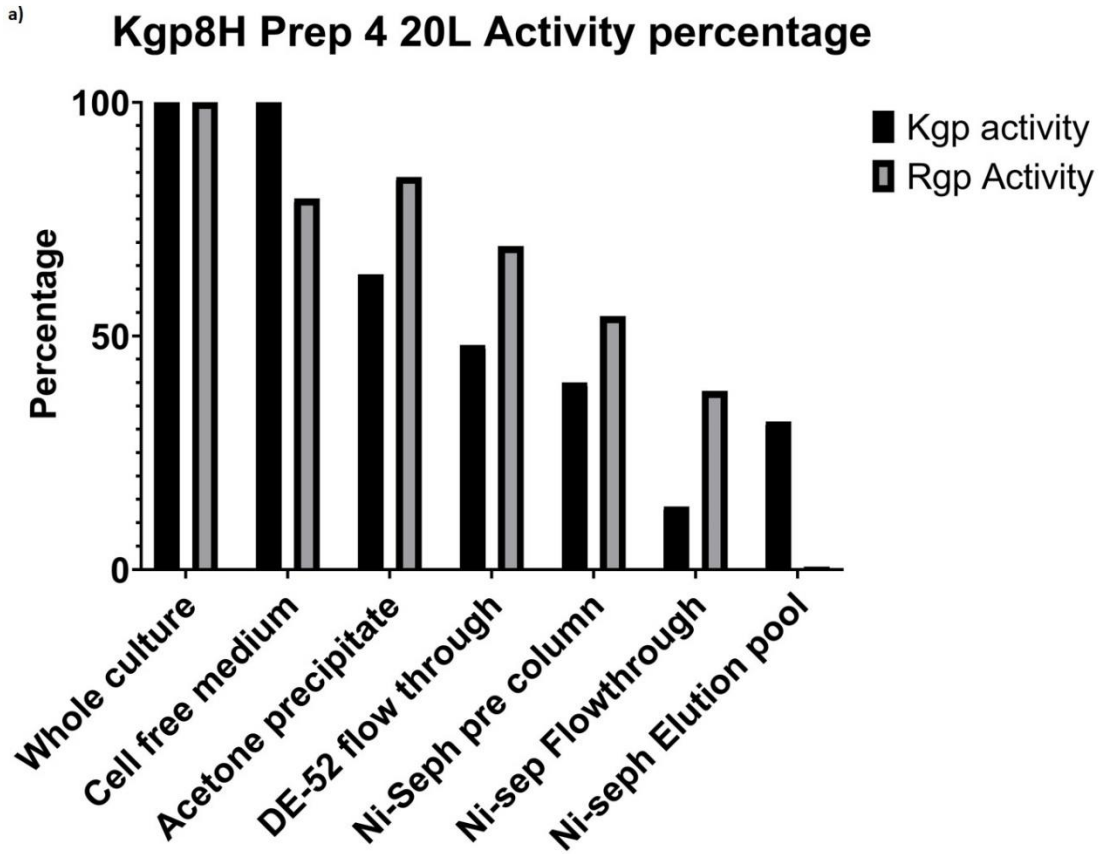


Figure 12- a) Retained activity of Kgp and Rgp at each stage of purification as a percentage of whole cell culture (WCC). western blot analysis of purified Kgp8H for b) anti-HA c) anti-6xHis and d) anti-Kgp reveals the presence of the repeated HA motif, His tag at low molecular weight, and catalytic domain at expected molecular weight.

Further investigation of the insoluble solids revealed that sonication was not sufficient to resolubilize the Kgp activity. This insolubility problem resulted in large drops in recovered Kgp activity at the acetone precipitation stage, 45% recovery compared to the 70% recovery for Rgp averaged amongst the large-scale preps, as well as at the DE-52 chromatography stage. After application on the DE-52 media, Kgp average activity recovery dropped to 25%, compared to the 50% average recovery for Rgp activity.

The second issue that arose was the apparent instability of the secreted Kgp from this mutant. Gingipains purified from wild-type or other mutants are stable for months when stored at -20°C and years when stored at -80°C . Gingipain activity will remain stable throughout the normal timeframe a large-scale purification takes. In the later large-scale preps for Kgp8H, the activity for Kgp would rapidly degrade from process samples stored at 4°C for even a few days. Further investigation revealed that acetone precipitation pellet samples dialyzed to ion exchange buffer then frozen at -20° for 7 days lost 25% Kgp activity, while Rgp activity remained unchanged. Elution samples from nickel-Sepharose stored at -80°C showed unchanged Kgp activity.

To further investigate these issues, a series of three small-scale purifications were planned, for 2L each. The issues were even more pronounced in these later purifications, showing a ~25% loss of Kgp activity at the pellet resolubilization stage and a further ~30% loss after the DE-52 application, averaged across all three purifications. The degradation issue was also observed, with whole cell culture samples taken from all three purifications losing

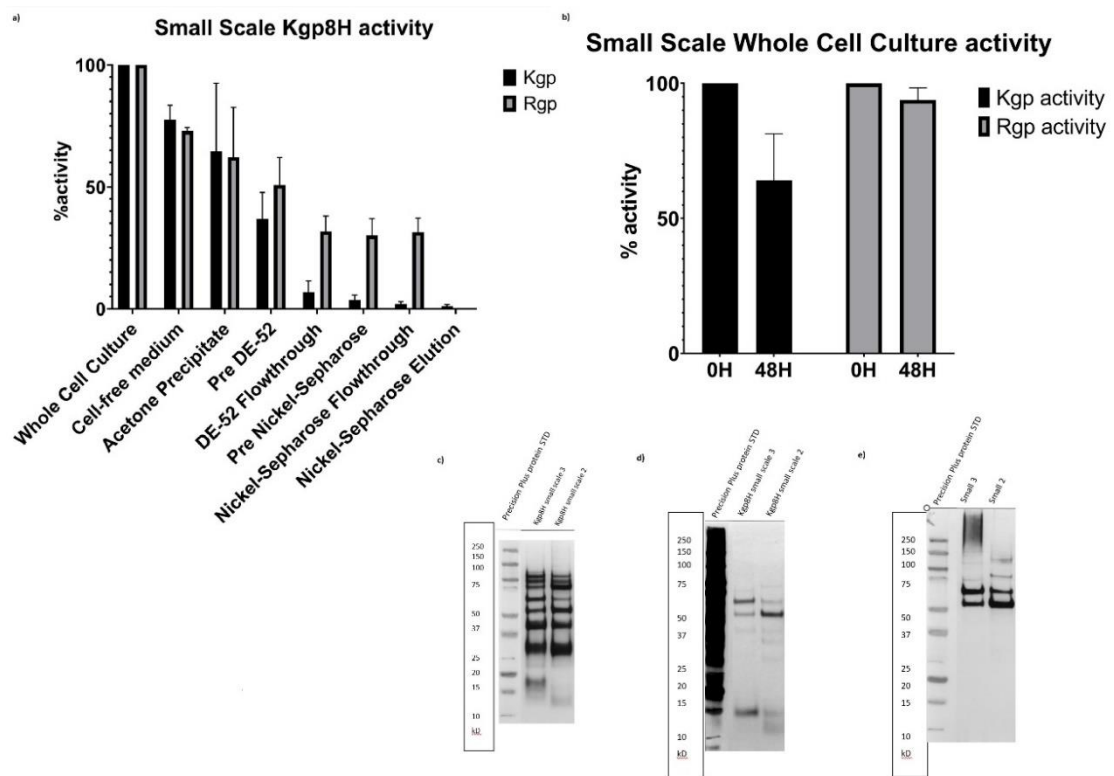


Figure 13- a) Retained Kgp and Rgp activity, averaged across all small-scale purifications, at each stage of purification as percentage of WCC. b) Kgp and Rgp activity of WCC at 0H and 48H timepoints after storage in 4°C indicates a ~35% loss of Kgp activity while Rgp activity remains unchanged. Western blot of Ni-Sepharose eluate from small scale preps with c) anti-HA, d) anti-6xHis e) anti-Kgp indicate substantially more degradation banding patterns than previous large scale purification blots, as well as degradation of the catalytic domain. His tag was also detected in large weight (~50kDa) c-terminal bands with degradation patterns.

an average of 35% Kgp activity after 48 hours stored at 4°C. Averaged yield was 0.219 mg or 0.109 mg/L culture. Western blot analysis showed evidence of

degradation in banding patterns of anti-HA and anti-Kgp, as well as different degradation patterns between small-scale preps (Figure 13).

W83 Δ Kgp RgpB8HTSI (RgpB8H)

This mutant was designed as a source for RgpB free from Kgp activity. The background strain used was W83 with the Kgp gene deleted, then a tag insertion was made at the same point as the previous RgpB mutant strain, 662, N-terminal of the TSI motif. An 8-His repeat tag was used to potentially prevent His-tag truncation seen in other mutants.

The initial large-scale purification was 10 liters total and performed according to standard protein purification protocol. After purification, protein

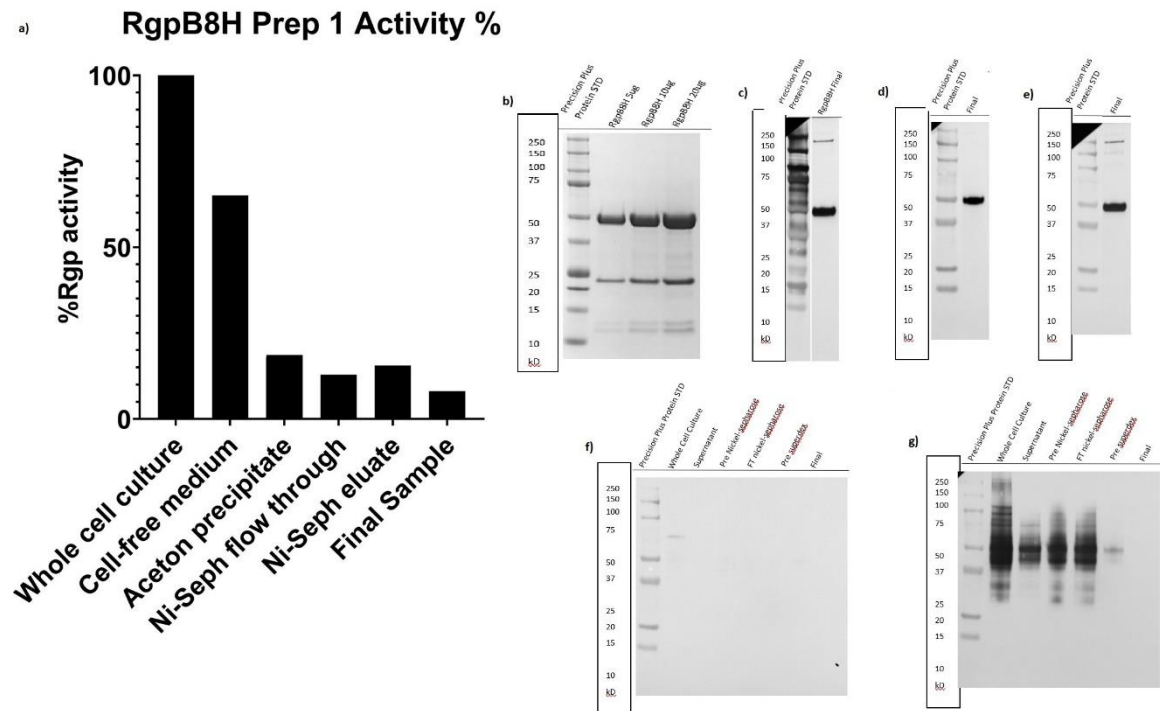


Figure 14 -a) Retained Rgp activity at each purification stage as a percentage of whole cell culture total activity. B) SDS-PAGE of final RgpB8H purified protein shows evidence of profragment at ~32kDa as well as cleavage products at ~12-13kDa. Western blot on final RgpB8H purified sample for c) anti-His d) anti-RgpB e) anti-Rgp f) anti-Kgp and g) anti-HA confirmed the successful insertion and purification of His tag on the ~50kDa catalytic domain, the ability of the purification process to remove the HA domains, and consequently the RgpA complex, from the final sample, and the success of the Δ Kgp mutation to silence expression of Kgp.

samples were characterized by activity assay, SDS-PAGE, and western blot (Figure 14). Western blot analysis showed single band RgpB with His-tag attached, as expected. Blotting confirmed the absence of Kgp as well as the ability of the purification process to separate out the HA domains associated with RgpA. A ~23 kDa band remains associated with the purified RgpB8H in the SDS-PAGE, which is the profragment normally degraded during the maturation process. The profragment is only partially inhibiting the gingipain proteolytic activity, with the final purified sample possessing about 60% specific activity compared to samples purified from the RgpB6H mutant. Final yield from this large-scale prep was 22 mg, or 2.2 mg/L culture. This was a comparable yield to the previous RgpB6H mutant, which averaged 2-2.5 mg/L culture.

To further investigate the presence of the profragment in samples purified from RgpB8H, a series of three small-scale purifications was performed. Each small-scale purification was 2L total culture volume and all three were run in parallel. Purification activity recovery of small scale was comparable to large scale purification (Figure 15). Averaged yield of purified protein was 2.68 mg/L. Final protein samples purified from small scale cultures also showed partial inhibition from retained profragment inhibitors. Purified RgpB8H with the profragment was incubated together with previously purified Kgp at 37°C for one hour. After incubation, the profragment band had been completely degraded, and Rgp activity increased over threefold (Figure 16).

RgpB8H Small Scale Activity % recovery

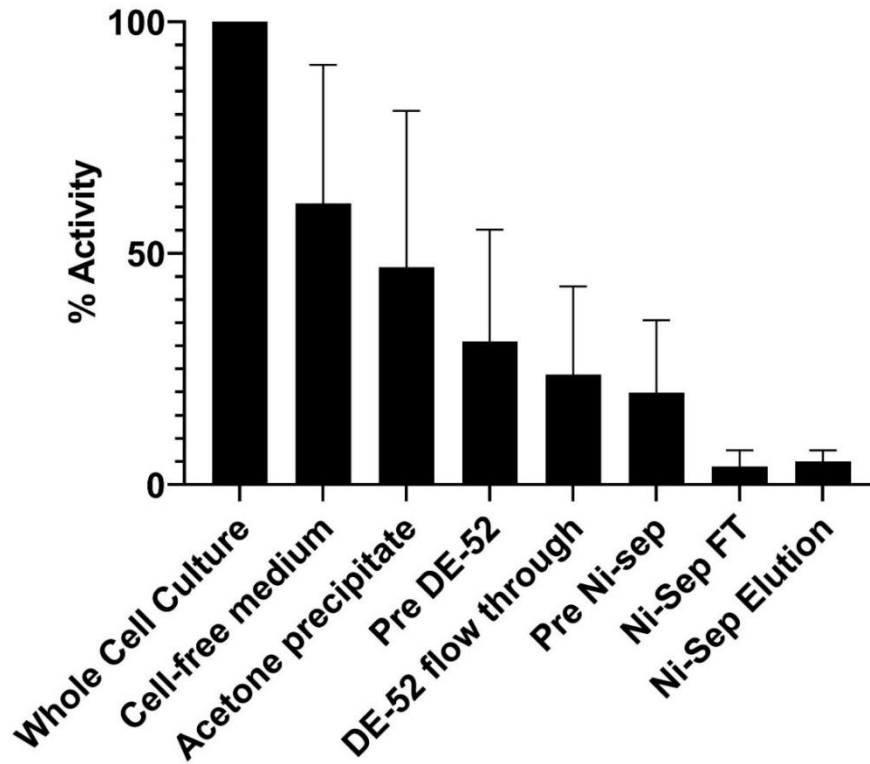


Figure 15— Averaged Rgp activity recovery at each stage of purification for small scale cultures.

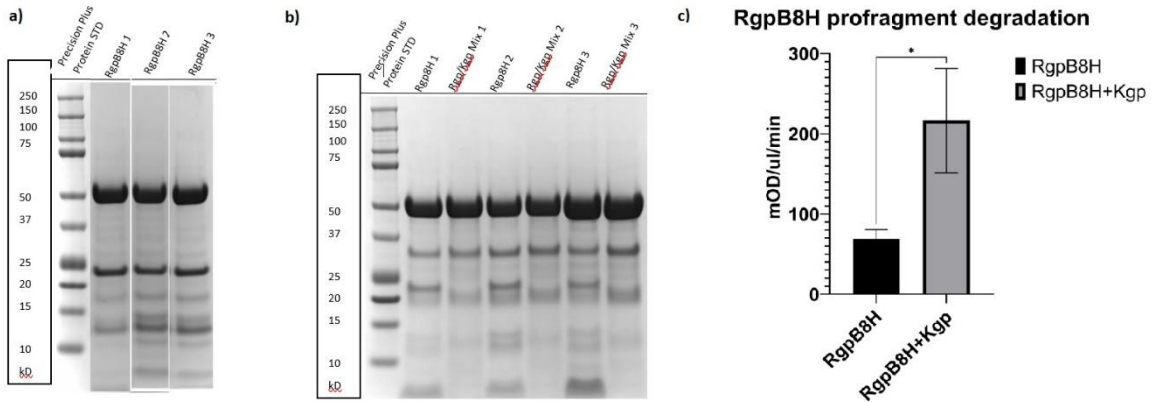
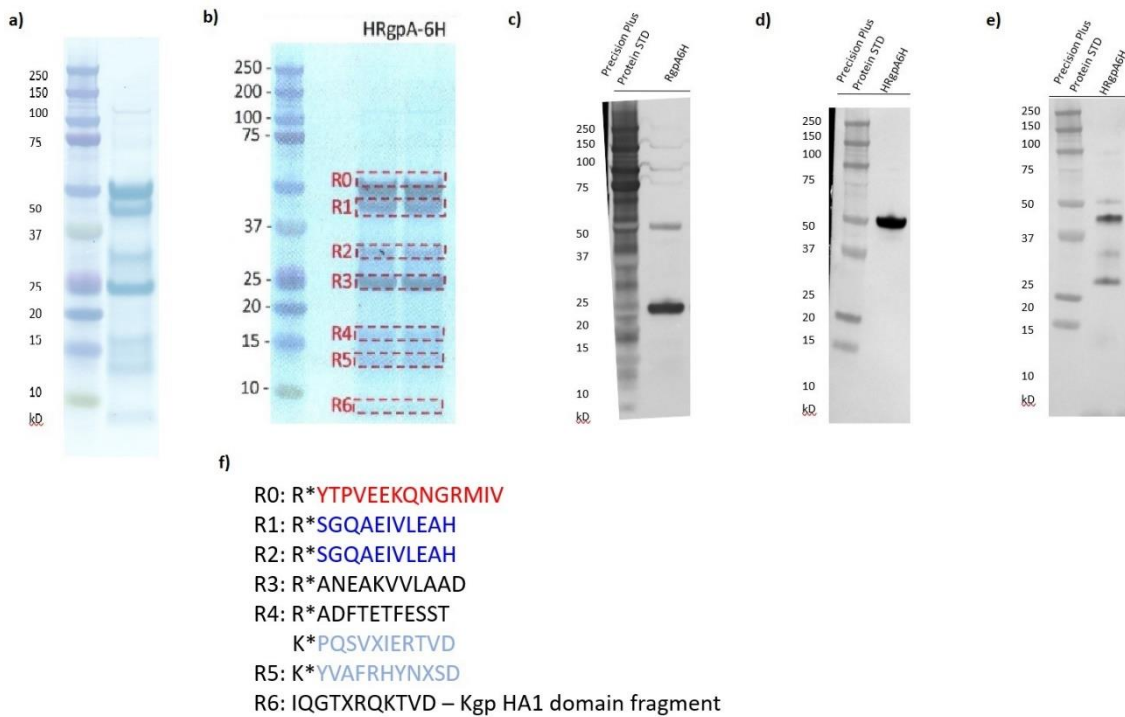


Figure 16— a) SDS-PAGE analysis of final RgpB8H from small scale purifications. b) SDS-PAGE analysis of RgpB8H samples alone or mixed with purified Kgp incubated for 1 hour at 37°C. Profragment band at ~23kDa is degraded in samples mixed with Kgp. c) Rgp activity of RgpB8H samples increased threefold after incubation with Kgp.

W83 Δ WBPB RGPA-YIP6HIS (RGPA6H)

This mutant was designed as a source for full-length RgpA, or “heavy RgpA” (HRgpA). The background strain for this mutant deleted the previously identified WbpB gene in W83 to prevent synthesis of A-LPS and consequently secrete all T9SS cargo proteins, including HRgpA, into the extracellular space. A six-histidine affinity tag was inserted into the gene for RgpA C-terminal to the YIP motif in the final HA domain, one residue N-terminal of the CTD cleavage residue. To investigate mutant viability, a 1L pilot culture was processed and RgpA6H was purified for analysis. Western blot confirmed the presence of the intact His tag at the HA4 domain, RgpA catalytic domain, and HA domains. Blotting for His tag identified the HA4 domain insertion around 23kDa; however, a signal at 50kDa also developed, likely a result of processing in the HA1 domain. Anti-HA blotting showed several bands reactive for the recurring motif, but the molecular weights do not all match with the expected domains. The presence of several more bands than recurrent motifs in the RgpA gene indicates processing outside canonical domain structures. Purified RgpA6H was analyzed by N-terminal sequencing to determine sequence of processed domains (Figure 17). Sequences for each expected domain were confirmed; however, two sequences for N-terminus of HA3 may indicate aberrant processing. Final yield of purified RgpA6H was 0.3 mg/L with an activity recovery of 1.6%.



g)

RgpA (W83)
 mknlnkfvslalcssllggmafaQQTELGRRNPVRLLESTQQSVTKVQFRMDNLKFTVQTPKGIGQVPTYTE
 GVNLSSEKMPPTLPILSRSLAVSDTREMKVEVSSKFIKKNVLIAPSKGMIMRNEDPKPIPYVYGKTYSONKF
 FPGEIATLDDPPILRDVRRGQVNVNFAPLQYNPVTKTLRIYTEITVAVSETSEQGNILNKKGTFFAGFEDTYKRM
 FMNYEPGR**YTPVEEKQNGRMIV**IVAKKYEGDIKDFVDWKNQRGLRTEVKVAEDIASPTANAIQQFVKQYEYK
 EGNDLTYVLLIGDHKDIPAKITPGIKSDQVYGGIVGNDHYNEVFIFGRFSCESKEDLKTQIDRTIHYERNITTE
 DKWLQALCIAASAEGGPSADNGESDIQHENVIANLLTQYGYTKI IKCYDPGVTPKNI IDAFNGGISLANYTGH
 GSETAWGTSHFGTTHVKQLTNSNQLPFI FDVACVNGDFLFSMPCFAEALMRAQKDGKPTGTVAIIASTINQSW
 ASPMRGQDEMNEILCEKHPNNIKRTFGGVTMNGMFAMVEKYKDGKMLDWTWVFGDPSLLVRTLVP TKMQVT
 APAQINLTDASVNVSCDYNGAIATISANGKMFSGSAVVENGATINLTLGLTNESTLTLTVVGYNKETVIKTI
 NGEPNPYQPVSNLTATQGGQVTLKWDAPSTKtattntarsvdgirelvllsvsdapellr**SGQAEIVLEAH**
 DVWNDGSGYQIILLDADHDQYQVIPS DHTLWPNCSPANLFAPEYTVPENADPSCSPTNMIIMDGTASVNI P
 AGTYDFAIAAPQANAKIWIAGQGPTEKEDDYVFEAGKKYHFLMKKMGSGDGTETLISEGGSDYTYTVYRDGK
 IKEGLTATTFEEDGVATGNHEYCVEVKYTAGVSPKVC KDVTVEGSNEFAPVQNL TGSVAVGQVTLKWDAPNGT
 PNPNPNNPNPNPGTTLSESFENGIPASWKTIDADGDGHGWKPGNAPGIAGYNSNGCVYSESFGLGGIGVLT
 PDNYLITPALDL PNGGKLTFWVCAQDANYASEHYAVYASSTGN DASNFTNALLEETITAKgvr speamrgr iq
 gtwrqtvdldpagtkyavfrhfqstmdfyidldeveikangkr**ADFTETFESST**HGEAPAWEWTTIDADGDGQG
 WLCSSGQLDWLTAHGGTNVSSFSWNGMALNPDNYLISKDVTGATKVYYAVNDGFPGDHYAVMISKTGTN
 AGDFTVVFEEPTNGINKggarfglsteadgak**QSVWIERTVD**LPAGTKY**VAFRHYNCSD**LNLYILLDDIQFTM
 GGSPTPTDYTYTVYRDGTKIKEGLTETTTFEEDGVATGNHEYCVEVKYTAGVSPKCVNVTVNSTQFNPVKNLK
 AQPDDGDDVVLKWEAPSAKktegsrevkrigdgltiepandv**ANEAKVLLAAD**NVWGDNTGYQLLADHN
 TFGSVIPATGPLFTGTASSDLYSANFESLIPANADPVVTTQNIIVTGQGEVVI PGGVYDYCITNPEPASGKM
 IAGDGGNQPARYDDFTFEAGKKYTFMRRAGMGDGT DMEVEDD SPASYTYTVYRDGTKIKEGLTETTYRDAGM
 SAQSHCYCVEVKYTAGVSPKVCVDYIPHHHHHHDgvadvtaqkpytlttvvgkttvtcqqeamiydmnrrla
 Agrntvvytaqgggyavmvvvdgksyveklaiik

Figure 17 Initial purification data of RgpA6H. a) SDS-PAGE banding of purified RgpA6H indicated purification of multi-band complex b) Highlighted bands were analyzed by N-terminal sequencing. Western blot analysis of purified RgpA6H for c) anti-6xHis d) anti-RgpA e) anti-HA. Anti-His showed an unexpected band at 50kDa. Anti-HA showed heterologous processing of detected HA motifs. f) N-terminal sequences from analyzed bands with * denoting cleavage site. g) Full amino acid sequence of RgpA gene from RgpA6H. N-terminal sequences in bold. Putative domains in differing colors. Lowercase indicates residues canonically lost during the maturation process. Anti-HA motif sequences are underlined.

Next, two large scale 20-liter purifications of RgpA6H were performed and

analyzed. The final yield for these purifications was a 0.4% and 0.49% Rgp activity recovery, 3.42mg and 4.66mg or 0.171mg/L and 0.233mg/L, respectively. The transition to large scale purification appeared to have lowered the ability of affinity matrix to purify RgpA6H, so a series of small-scale purifications was performed. Three one-liter purifications were performed, with final yields of 0.81mg, 1.06mg, and 0.78mg, for an average yield of 0.883mg/L. A further set of three two-liter purifications was performed; however, after affinity chromatography no proteins were eluted. Analysis of the protein sample that was loaded onto the nickel-Sepharose column showed that 4-6 histidine repeats could not be detected in any of the three two-liter small scale samples (Figure 18).

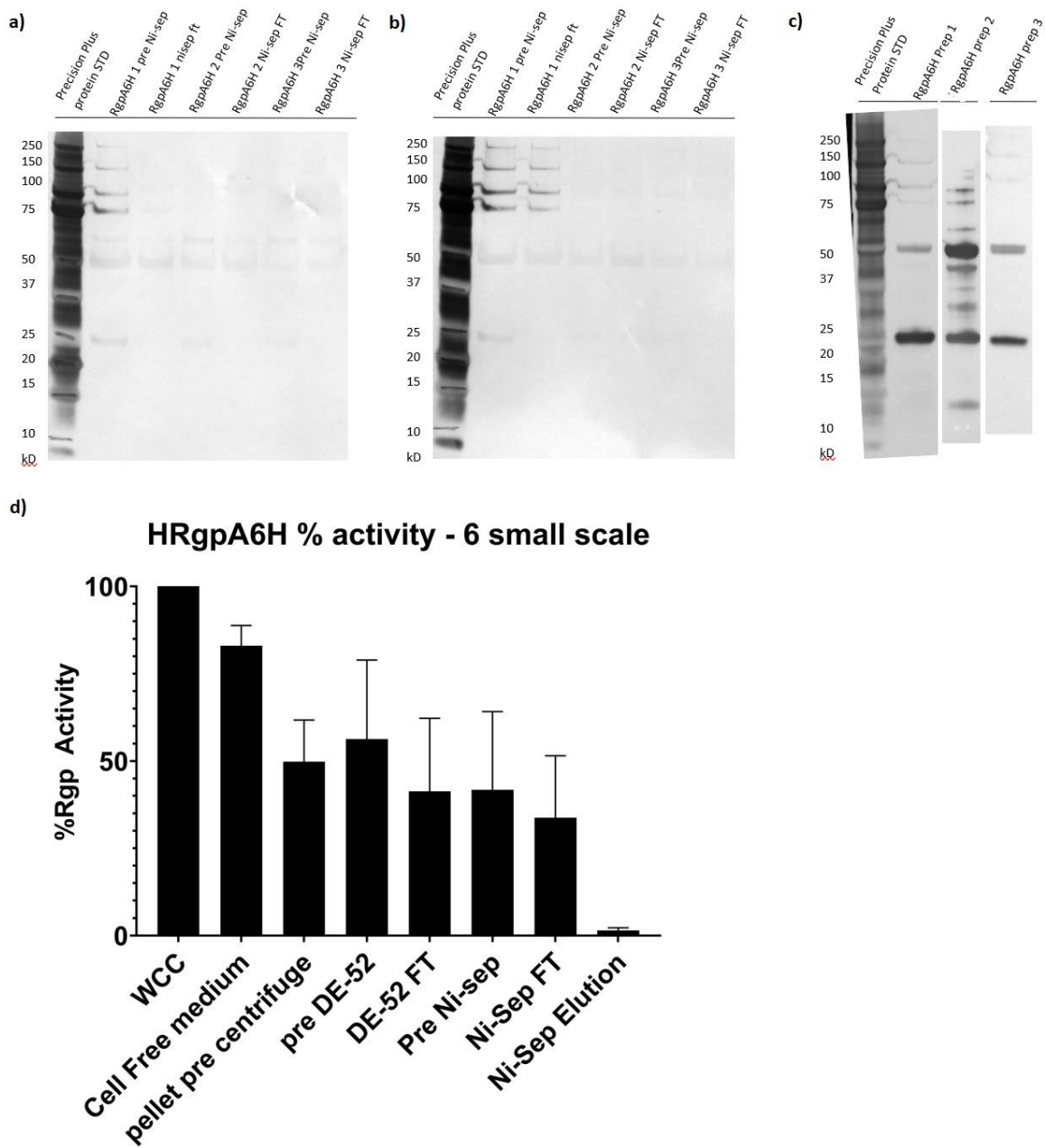


Figure 18 – Western blot analysis for samples before and after nickel-sepharose affinity purification for three small scale preps against a) anti 4-6xhis b) anti-6xhis and. c) anti-6xhis for large scale purifications 1-3 indicates loss of the His affinity tag in later purifications compared to the earlier preps. D) Average Rgp activity recovery for 6 small scale purifications.

DISCUSSION

The overall objective of this project was to determine the viability of three mutants to produce their engineered gingipains in large-scale quantities, and then to characterize those products. Each mutant was created to generate a single purifiable gingipain and was selected for its apparent success at producing a soluble gingipain with an affinity tag. Transitioning to large-scale purifications presents unique challenges, and mutants that appear viable in initial low-volume cultures may not remain so after subsequent passaging and large-scale purification. Ultimately, Kgp8H and RgpA6H are non-viable for gingipain purification, while RgpB8H is a viable source for Kgp-free RgpB, with a significant deviation from wild type with partial profragment retention.

Kgp8H was an initially promising candidate that seemed successful in producing full-length Kgp, a result that had remained elusive to this point. The initial purification was confirmed with a novel antibody for a recurring motif in the HA domains, showing the HA domains were retained, and sequencing data revealed the N-terminal starting residues for each band. This appeared to have successfully purified the HA domains along with the catalytic domain at first glance. Further investigation revealed several bands with N-terminal cleavage sites that did not have arginine or lysine at the P1 position, which is not a

common result in *P. gingivalis*. Additionally, the presence of the His-tag band at ~50kDa also indicates a likely arginine cleavage site in the middle of the HA1 domain that is not processed further, leaving a 50kDa polypeptide. The presence of several bands binding mAb reactive to the YTYTVYRDG recurring motif also indicates cleavage patterns that do not strictly adhere to the canonical HA domain regions. There were three strongly reactive bands for two recurring motifs in the Kgp gene, so there must be some heterologous proteolytic processing affecting HA domains. The lack of sequencing results for the N-terminus of HA2 and HA3 also indicated that the domain maturation and processing of Kgp had significantly diverted from wild type enzymes.

In subsequent large-scale purifications, it became apparent that a large portion of secreted Kgp8H was becoming insoluble after acetone precipitation, then lost in later purification steps. This white precipitate did not seem to be aggregate or readily resolvable; however, not all soluble Kgp activity was affected. Centrifuging after the protein pellet dialysis is required to remove unwanted insoluble materials, however due to the solubility issue of Kgp in this mutant, significant amounts of target proteins also were lost. After protein pellet dialysis, the resulting sample is loaded onto DE-52 matrix, which in addition to functioning as an ion-exchange chromatography matrix is also the first stage where the sample is mechanically filtered. Again, due to the solubility issue, further significant amounts of Kgp activity were lost at this stage where the enzyme should not be retained.

Also observed in these large-scale purifications was rapid losses of Kgp activity, sometimes even after only days of storage at 4°C, an environment where gingipains are usually stable for months to years. These losses were evident in repeated activity assays of samples at the cell-free media and acetone precipitate stages, and occurred even in samples that were stored for 7 days at -20°C. However, samples at later steps of purification, after removal of Rgp activity, did not exhibit the same degradation. Taken together with the banding patterns seen in the western blots, it appears Rgp cleavage activity is degrading the Kgp8H produced by this mutant at residues not expected in the wild-type. As the maturation process of gingipains has not been fully elucidated at the time of writing, it is difficult to speculate what may have changed in this mutant to expose arginine residues not typically cleaved to this proteolytic activity. One possibility is the insertion of the His-tag interfered with the normal folding process of the gingipain, and the resulting structure may have exposed normally protected arginine residues. This structural change could also explain the precipitation if the abnormal structure was further modified by the acetone precipitation into a completely insoluble configuration.

Overall, the two issues of solubility and stability make Kgp8H mutant not viable for large-scale purification. The stability issue is incompatible with the time required for large-scale purifications, further compounded by the large yield losses caused by the insolubility. These issues may have been exacerbated by mutations incurred by repeated passaging; however, even the characterization data obtained from the initial purification has some evidence of degradation. A

new insertion point for affinity tag in a new mutant is a better option for purification of full-length Kgp than attempting to solve both stability and solubility issues in this mutant.

The RgpB8H mutant was designed as a source of RgpB activity free from any Kgp contamination. This goal was met, as all RgpB8H purified from this mutant did not have even trace levels of Kgp activity. The mutant transitioned to large-scale purification well and produced yields comparable to the previous RgpB mutant. The proteolytic activity of RgpB8H is affected by the incomplete clearance of the inhibitory profragment, but enough activity remains to be a viable source of RgpB. The partial inhibition and presence of cleavage products indicate that Kgp plays some role in the proper clearance of the profragment, confirmed by incubation of purified RgpB8H with previously purified Kgp. RgpB8H mutant is an excellent option for experiments where Rgp activity free from any Kgp activity is critical.

RgpA6H mutant was generated as a source of full-length RgpA, which has been difficult to isolate in the past. By insertion of the His affinity tag, RgpA could be collected in large quantities and high purities from large-scale purifications. The mutant initially produced RgpA with affinity tag, although the yields were relatively low. This was acceptable as a novel source of RgpA as any amount produced was valuable. However, successive purifications showed declining yields, eventually producing no soluble RgpA with a detectable His affinity tag. This tag truncation has been seen in previous mutants for the Kgp gene yet the exact mechanism of tag truncation remains unknown. It is more likely to be a

post-translational modification of the produced protein rather than a mutation of the gene sequence; however, sequencing of the genome is necessary to confirm. With the tag truncation occurring after several rounds of passaging, it is likely that some compensatory mutation was developed by *P. gingivalis* to affect the tag. Without the attached His tag, this mutant secretes all T9SS cargo proteins into the extracellular space, essentially an analog for the wild-type HG66 strain. The mutant could be remade and maintained with careful regulation of passages to theoretically maintain the His-tag. Without addressing the underlying mechanism of tag truncation, this unknown mechanism would still be present and eventually become problematic at some point in the future.

FUTURE WORK

The truncation of the RgpA His tag seems to be the result of some unknown mechanism utilized by *P. gingivalis*. To further investigate the effects in the RgpA mutant, we plan to sequence the gene for RgpA to ensure that the affinity tag insertion is still intact, and then sequence the whole genome to screen for potential compensatory mutations. If any are present, it may lead to a better understanding of the mechanisms of affinity tag truncation and allow for methods for circumvention. If the truncation issue can be fixed or mitigated, purified full length RgpA will be used for x-ray crystallography, to solve the structure of the HA domains and to further investigate the hemagglutinin and adhesin activities of those domains.

Kgp8H had multiple problems that prevented success as a protein production candidate. We plan to sequence the Kgp gene to verify that the insertion remains intact, then sequence the whole genome to screen for compensatory mutations. While this mutant does not produce intact full-length Kgp as hoped, it may be useful in investigating the gingipain maturation process as a case where maturation was disrupted.

The presence of partially processed but undegraded profragment in purified RgpB8H may provide some insights into profragment degradation in wild

type gingipains. Sequencing the profragment band as well as the potential degradation bands could identify an initial cleavage point for total profragment degradation.

MATERIALS AND METHODS

PROTEIN PURIFICATION

MATERIALS

- Anaerobic chamber/jars filled 90% (v/v) N₂, 5% (v/v) CO₂ 5% (v/v) H₂ gas mix
- Liquid growth media - enriched trypticase soy broth (eTSB) per 1L:
- 30g trypticase soy broth (Sigma T8907), 10g yeast extract (Gibco 212750), autoclave sterilize then add filter sterilized 5ug/ml Hemin (Sigma H9039), 0.25mg/ml L-cysteine (Spectrum CY110) and 0.5ug/ml Menadione (Sigma M5625).
- Dithiodipyridine (Arcos 162240250)
- Dithiodipyridine buffer (20mM Bis-Tris, 150mM NaCl, 1.5mM 4,4' - Dithiodipyridine, 0.02% NaN₃, pH 6.8)
- DE-52 anion-exchange matrix (Biophoretics B45059.02)
- Blood agar plates – prepare eTSB with 1.5% agar (VWR J637), autoclave sterile then add filter sterilized Hemin, L-cysteine, Menadione, 20% (v/v)

- blood (Defibrinated sheep, Lampire 7239001), and selective antibiotics, if applicable. Acetone (Fisher A949-4)
- Nickel-Sepharose 6 fast flow matrix (GE 17-5318-03)
- Flat bottom 2.8L flask and container
- Sorvall Evolution RC Refrigerated centrifuge with Sorvall SLC-3000 rotor or equivalent
- Sorvall Lynx 6000 Refrigerated Centrifuge with F9-6x1000 rotor or equivalent
- Centrifuge bottle 400ml PPCO Thermo 3141-0500
- Centrifuge bottle 1000ml PPCO Thermo 010-1491
- Ion-exchange buffer: 50mM Bis-Tris, 5mM CaCl₂, 0.02% NaN₃ pH 6.5
- Nickel-Sepharose binding buffer: (20mM Na₂HPO₄, 500mM NaCl, 20mM imidazole, 0.02% NaN₃, pH 7.4)
- Nickel-Sepharose elution buffer: (20mM Na₂HPO₄, 500mM NaCl, 500mM imidazole, 0.02% NaN₃, pH 7.4)
- Fractionation machine (Pharmacia Biotech GradiFrac 18-1993-01)
- Dry Ice
- Cytiva AKTA go FPLC system
- HiLoad 16/60 Superdex 200 pg column (GE healthcare 17-1069-01)
- Dialysis bag (Spectra/Por standard RC tubing 12-14kD mwco 132754)

- Amicon stirred cell concentrator VFSC40001
- Concentrator membrane (Biomax 30kDa PBTK07610)
- Spectrophotometer (molecular devices Spectramax m5)
- Stir plate/Stir bars
- Separatory funnel with stand and clamps
- Final gingipain buffer (20mM Bis-Tris, 150mM NaCl, 5mM CaCl₂, 0.02% NaN₃ pH 6.8)

METHOD

Purification of gingipains followed a modified version of protocol previously described⁴¹. *P. gingivalis* bacterial stocks stored at -80°C were revitalized in 5mL selective eTSB and grown in anaerobic conditions for 2-3 days, until absorbance measured at 600nm (OD₆₀₀) reached 1.3 to 1.5. Culture was then plated on blood agar plates selective for each strain's resistances and incubated for 5-7 days until single colonies were able to be collected. Single colonies were cultured in 5 mL selective eTSB in anaerobic conditions for 2-3 days to OD₆₀₀ 1.3-1.5, then 1mL grown culture was used to seed 50mL selective eTSB and grown for a further 2-3 days to OD₆₀₀ 1.3-1.5. Large scale cultures were seeded with 25-50mL seed per L of selective eTSB media and grown 3-4 days until reaching OD₆₀₀ 1.3-1.5. Assay for gingipain activity was performed at each grown culture step to verify strain viability according to assay protocol. Grown culture was centrifuged at 10000g for 30 min 4°C to separate cells from

culture medium. Medium was collected, kept at 4°C, and 1.5mM Dithiodipyridine was added.

Assembly of acetone precipitation apparatus consisted of stir plate, container with flat bottom 2.8L flask on top, large stir bar in flask, and stand holding separatory funnel over opening of flask. *P. gingivalis* collected medium was added to flask, then prechilled (-20°C O/N) acetone was added to the separatory funnel and added dropwise to the flask in a 60% (v/v) ratio (1.5L acetone to 1L medium). Dry ice was packed into container outside flask to keep flask chilled during precipitation. 30-minute precipitation started when all acetone was added, and sample vigorously stirred to prevent icing. Precipitate solution was centrifuged at 17568g for 30 min at 4°C. Pellets were collected and resuspended in Dithiodipyridine buffer, stirred to homogenize, then dialyzed in 4L Dithiodipyridine buffer at 4°C overnight. Dialysis bag was transferred to series of 4 4L ion exchange buffers and dialyzed at 4°C for 4 hours each. After dialysis the sample was centrifuged 10000g at 4°C for 30 minutes then concentrated on Amicon concentrator with 30k mwco membrane in 4°C. Sample was then loaded 2x gravity on 50 mL bed volume DE-52 matrix equilibrated in ion exchange buffer and column flowthrough was collected. Sample was then dialyzed 4 times to 4L Nickel-Sepharose binding buffers at 4°C for 4 hours. A 10mL bed volume nickel-Sepharose column was prepared and equilibrated with Ni-Sep binding buffer, then sample was applied to column by 2x gravity. Column was washed with ni-sep binding buffer until absorbance at 280nm

was <0.02. Ni-sep elution buffer was applied to column and fractions were collected with fractionation machine. Fractions were assayed for gingipain activity and pooled together, then pools were concentrated with 30k MWCO spin concentrators. Sample was dialyzed to final gingipain buffer 4 4L for 4 hours each at 4°C. Protein sample was run on FPLC system with HiLoad Superdex 200 16/60 column for size exclusion, flow rate 0.75mL/min in final gingipain buffer and 1mL fraction size. Fractions were assayed for gingipain activity and pooled together for final sample.

GINGIPAIN ACTIVITY ASSAY

MATERIALS

- Gingipain assay buffer (200mM Tris, 150mM NaCl, 5mM CaCl₂, 0.02% NaN₃ pH 7.6)
- 1M L-Cysteine stock (Spectrum CY110)
- 96 well clear plate (Corning Costar 9017)
- Spectrophotometer (molecular devices Spectramax m5)
- Rgp substrate: Bz-arg-pNA (Bachem 4000792.0250)
- Kgp substrate: Ac-lys-pNA (Bachem 4004444.0250)
- Dimethylsulfoxide (DMSO) (Sigma 472301)

METHOD

Gingipain substrates must be reconstituted in DMSO for solubility to a stock concentration of 200mM or 500mM. Substrates must be further

diluted in DMSO for assay working concentration of 20mM. Absorbance readings will be taken with shaking at A_{280} every 30 seconds for a period of 10 minutes at 37°C. Assay scheme must be planned such that total well volume of buffer, substrate, and sample equals 200uL. Sample volume must be adjusted such that the kinetic curve over 10 minutes is within the range of spectrophotometer reading limits. Assay buffer must be activated with 20mM L-cysteine and is viable for 4 hours after activation. Activated buffer is first added to each well, then sample is added to buffer. Substrate is added to each well to bring total volume to 200uL, then spectrophotometer readings are immediately started. Final K_{max} reading is divided by volume of sample used and gives final unit value of mOD/ul/min for gingipain activity.

SDS-PAGE

MATERIALS

- Precast 4-12% Bis-tris polyacrylamide gel (Invitrogen NuPAGE NP0335BOX)
- B-mercaptoethanol (BME) (Sigma M-7522)
- Na-tosyl-L-lysine chloromethyl ketone (TLCK) (Sigma T7254)
- Sample buffer (Invitrogen NuPAGE LDS sample buffer 1941674)
- Heat block capable of 100°C
- X-cell surelock electrophoresis system (Invitrogen novex)

- Power supply (Bio-rad powerPac 300)
- SDS running buffer (Invitrogen NuPAGE MES SDS NP0002-02)
- Molecular mass protein standard (Precision plus Protein Standards, BioRad)
- Blue safe stain (Novex SimplyBlue SafeStain LC6065)
- Microwave
- Rocking shaker (VWR 10127-876)

METHOD

Samples were incubated with 2ul of 200mM TLCK for 10 minutes at room temperature. Reduced samples added 5µl NuPAGE loading buffer and incubated 5 min at 100°C, then added 5µl NuPAGE loading buffer with 10% BME (Sigma M-7522) and the samples heated at 100°C for 5 additional minutes. Samples were electrophoresed on 4-12% Bis-Tris SDS-PAGE (Invitrogen NP0335BOX) at 160 volts for 60 minutes. Gel was stained with SimplyBlue stain and heated in microwave for 1 min, then incubated for 1 hr. on rocking shaker. Stain was then discarded, and gel was heated in microwave in dH₂O for 2 minutes, then incubated for 2 hours to de-stain.

WESTERN BLOT

MATERIALS

- Nitrocellulose membrane (Biorad 162-0116)
- Sponge Pads (Invitrogen EL9052)
- Filter paper (Whatman 3 1003-917)
- Bio-Rad mini PROTEAN 3 cell
- Transfer buffer (25mM Tris, 192mM Glycine, 20% methanol)
- Ice pack
- Ice and container
- Power supply (Bio-Rad PowerPac 300)
- Milk (BioShop SKI400.500)
- Rocking shaker (VWR 10127-876)
- TTBS (20mM Tris, 150mM NaCl, 0.1% Tween-20 pH 7.5)
- A.P. conjugate substrate kit (Bio-rad 1706432)

METHOD

Followed SDS-PAGE method until gel run was finished before staining. Filled transfer assembly container with prechilled degassed (4°C) transfer buffer and soaked fiber pads, filter paper, gel, and nitrocellulose membrane. Assembled transfer sandwich from negative side: Fiber pad, filter, gel, membrane, filter, Fiber pad. Rolled transfer sandwich with roller to remove air bubbles before closure. Loaded transfer sandwich into

transfer assembly, added ice pack behind negative side, then filled assembly with chilled transfer buffer. Assembly placed in container surrounded with packed ice. Transfer performed at 100v for 60 min, then membrane stained with Ponceau S solution to check for successful transfer. Membrane blocked with 5% milk then incubated at R.T. for 1 hour with rocking. Membrane was then washed 3 times with TTBS for 5 minutes each with rocking, then incubated with primary antibodies overnight at room temperature with rocking. After washing 3 times with TTBS for 5 minutes with rocking, membrane was incubated with secondary antibodies for 2 hours at room temperature with rocking. Final wash of 4 times TTBS with 5-minute rocking was performed, then membrane was developed with alkaline phosphatase color development kit until signal was clear. Development was stopped by rinsing membrane with dH₂O.

IMAGING

MATERIALS

- Imager (Bio-Rad ChemiDOC XRS+)
- Software (Bio-Rad ImageLab 6.0)
- White light conversion screen (Bio-Rad 1708289)

METHOD

Polyacrylamide gels and western blot membranes were imaged with imager and associated software using presets for Coomassie blue protein gels and colorimetric blots, respectively.

MUTAGENESIS

Generation of the three mutant strains used in this project was performed in the Potempa lab at Jagiellonian University, Krakow, Poland. Kgp8H and RgpA6H were created by Danka Mizgalska. RgpB8H was created by Zuzanna Nowakowska.

REFERENCES

1. Lasica AM, Ksiazek M, Madej M, Potempa J. The Type IX Secretion System (T9SS): Highlights and Recent Insights into Its Structure and Function. *Frontiers in cellular and infection microbiology* 2017;7:215-15.
2. Nguyen K-A, Potempa J. Chapter 522 - Gingipain R. In: Rawlings ND, Salvesen G, editors. *Handbook of Proteolytic Enzymes (Third Edition)*: Academic Press; 2013. p. 2328-36.
3. Lamont R, Lewis J, Potempa J. Virulence Factors of Periodontal Bacteria. In: Lamont RH, G. Jenkinson, H., editor. *Oral Microbiology and Immunology*. 2nd ed. Washington, DC: ASM Press; 2013. p. 273-86.
4. Sztukowska M, Veillard F, Potempa B, et al. Disruption of gingipain oligomerization into non-covalent cell-surface attached complexes. *Biol Chem* 2012;393(9):971-7.
5. Pike RN, Potempa J. Chapter 523 - Gingipain K. In: Rawlings ND, Salvesen G, editors. *Handbook of Proteolytic Enzymes (Third Edition)*: Academic Press; 2013. p. 2337-44.
6. WHO. *Global oral health status report: towards universal health coverage for oral health by 2030*. Geneva: World Health Organization; 2022.
7. Kuo L-C, Polson AM, Kang T. Associations between periodontal diseases and systemic diseases: A review of the inter-relationships and interactions with diabetes, respiratory diseases, cardiovascular diseases and osteoporosis. *Public Health* 2008;122(4):417-33.
8. Bobetsis YA, Barros SP, Offenbacher S. Exploring the relationship between periodontal disease and pregnancy complications. *J Am Dent Assoc* 2006;137 Suppl:7s-13s.
9. Offenbacher S, Katz V, Fertik G, et al. Periodontal infection as a possible risk factor for preterm low birth weight. *J Periodontol* 1996;67(10 Suppl):1103-13.
10. López NJ, Smith PC, Gutierrez J. Periodontal therapy may reduce the risk of preterm low birth weight in women with periodontal disease: a randomized controlled trial. *J Periodontol* 2002;73(8):911-24.
11. Nibali L, D'Aiuto F, Griffiths G, et al. Severe periodontitis is associated with systemic inflammation and a dysmetabolic status: a case-control study. *J Clin Periodontol* 2007;34(11):931-7.
12. Bingham CO, 3rd, Moni M. Periodontal disease and rheumatoid arthritis: the evidence accumulates for complex pathobiologic interactions. *Curr Opin Rheumatol* 2013;25(3):345-53.
13. Kerschull M, Demmer RT, Papapanou PN. "Gum bug, leave my heart alone!"-- epidemiologic and mechanistic evidence linking periodontal infections and atherosclerosis. *J Dent Res* 2010;89(9):879-902.
14. Gao S, Li S, Ma Z, et al. Presence of *Porphyromonas gingivalis* in esophagus and its association with the clinicopathological characteristics and survival in patients with esophageal cancer. *Infect Agent Cancer* 2016;11:3.
15. Dominy SS, Lynch C, Ermini F, et al. *Porphyromonas gingivalis* in Alzheimer's disease brains: Evidence for disease causation and treatment with small-molecule inhibitors. *Sci Adv* 2019;5(1):eaau3333.
16. Socransky SS, Haffajee AD. Evidence of bacterial etiology: a historical perspective. *Periodontology* 2000 1994;5(1):7-25.

17. Socransky SS, Haffajee AD, Cugini MA, Smith C, Kent Jr. RL. Microbial complexes in subgingival plaque. *Journal of Clinical Periodontology* 1998;25(2):134-44.
18. Darveau RP. Periodontitis: a polymicrobial disruption of host homeostasis. *Nat Rev Microbiol* 2010;8(7):481-90.
19. Darveau RP, Hajishengallis G, Curtis MA. Porphyromonas gingivalis as a potential community activist for disease. *J Dent Res* 2012;91(9):816-20.
20. Green ER, Meccas J. Bacterial Secretion Systems: An Overview. *Microbiol Spectr* 2016;4(1).
21. Nguyen KA, Travis J, Potempa J. Does the importance of the C-terminal residues in the maturation of RgpB from Porphyromonas gingivalis reveal a novel mechanism for protein export in a subgroup of Gram-Negative bacteria? *J Bacteriol* 2007;189(3):833-43.
22. Zhou XY, Gao JL, Hunter N, Potempa J, Nguyen KA. Sequence-independent processing site of the C-terminal domain (CTD) influences maturation of the RgpB protease from Porphyromonas gingivalis. *Mol Microbiol* 2013;89(5):903-17.
23. Veillard F, Potempa B, Guo Y, et al. Purification and characterisation of recombinant His-tagged RgpB gingipain from Porphyromonas gingivalis. *Biol Chem* 2015;396(4):377-84.
24. Shoji M, Sato K, Yukitake H, Naito M, Nakayama K. Involvement of the Wbp pathway in the biosynthesis of Porphyromonas gingivalis lipopolysaccharide with anionic polysaccharide. *Sci Rep* 2014;4:5056.
25. Potempa J, Pike R, Travis J. Titration and Mapping of the Active Site of Cysteine Proteinases from Porphyromonas gingivalis (Gingipains) Using Peptidyl Chloromethanes. 1997;378(3-4):223-30.
26. Abdi K, Chen T, Klein BA, et al. Mechanisms by which Porphyromonas gingivalis evades innate immunity. *PLOS ONE* 2017;12(8):e0182164.
27. Olczak T, Dixon DW, Genco CA. Binding specificity of the Porphyromonas gingivalis heme and hemoglobin receptor HmuR, gingipain K, and gingipain R1 for heme, porphyrins, and metalloporphyrins. *Journal of bacteriology* 2001;183(19):5599-608.
28. Andrian E, Grenier D, Rouabhia M. In vitro models of tissue penetration and destruction by Porphyromonas gingivalis. *Infection and immunity* 2004;72(8):4689-98.
29. O'Brien-Simpson NM, Pathirana RD, Walker GD, Reynolds EC. Porphyromonas gingivalis RgpA-Kgp proteinase-adhesin complexes penetrate gingival tissue and induce proinflammatory cytokines or apoptosis in a concentration-dependent manner. *Infect Immun* 2009;77(3):1246-61.
30. Popadiak K, Potempa J, Riesbeck K, Blom AM. Biphasic effect of gingipains from Porphyromonas gingivalis on the human complement system. *J Immunol* 2007;178(11):7242-50.
31. Imamura T, Travis J, Potempa J. The biphasic virulence activities of gingipains: activation and inactivation of host proteins. *Curr Protein Pept Sci* 2003;4(6):443-50.
32. Rangarajan M, Smith SJ, U S, Curtis MA. Biochemical characterization of the arginine-specific proteases of Porphyromonas gingivalis W50 suggests a common precursor. *Biochem J* 1997;323 (Pt 3)(Pt 3):701-9.
33. Veillard F, Sztukowska M, Nowakowska Z, et al. Proteolytic processing and activation of gingipain zymogens secreted by T9SS of Porphyromonas gingivalis. *Biochimie* 2019;166:161-72.
34. Mikolajczyk-Pawlinska J, Kordula T, Pavloff N, et al. Genetic Variation of Porphyromonas gingivalis Genes Encoding Gingipains, Cysteine Proteinases with Arginine or Lysine Specificity. 1998;379(2):205-12.

35. Mahmud ASM, Seers CA, Huq NL, et al. Production and properties of adhesin-free gingipain proteinase RgpA. *Scientific Reports* 2023;13(1):10780.
36. Guo Y, Nguyen KA, Potempa J. Dichotomy of gingipains action as virulence factors: from cleaving substrates with the precision of a surgeon's knife to a meat chopper-like brutal degradation of proteins. *Periodontol 2000* 2010;54(1):15-44.
37. Jia L, Han N, Du J, et al. Pathogenesis of Important Virulence Factors of *Porphyromonas gingivalis* via Toll-Like Receptors. *Frontiers in Cellular and Infection Microbiology* 2019;9.
38. Fitzpatrick RE, Wijeyewickrema LC, Pike RN. The gingipains: scissors and glue of the periodontal pathogen, *Porphyromonas gingivalis*. *Future Microbiol* 2009;4(4):471-87.
39. Grenier D, La VD. Proteases of *Porphyromonas gingivalis* as important virulence factors in periodontal disease and potential targets for plant-derived compounds: a review article. *Curr Drug Targets* 2011;12(3):322-31.
40. Makyio H, Kato R. X-Ray Crystallography of Sugar Related Proteins. In: Taniguchi N, Endo T, Hart GW, Seeberger PH, Wong C-H, editors. *Glycoscience: Biology and Medicine*. Tokyo: Springer Japan; 2015. p. 175-82.
41. Potempa J, Nguyen KA. Purification and characterization of gingipains. *Curr Protoc Protein Sci* 2007;Chapter 21:Unit 21.20.
42. Hengen PN. Purification of His-Tag fusion proteins from *Escherichia coli*. *Trends in Biochemical Sciences* 1995;20(7):285-86.

CURRICULUM VITAE

Andrew E Fuchs
5516 Westhall Ave
Louisville, Ky 40214
(502) 552-3079

Andrew.fuchs@louisville.edu

Afuchs87@gmail.com

Summary:

I am a research technician pursuing a Master's of Science in Oral Biology degree. I have nearly 6 years of experience working in a biochemistry laboratory with focus in protein purification and characterization. My research interests are in interactions of the oral microbiome with systems outside the oral cavity, and how virulence is spread through the host.

Education:

2023 (Expected) **Oral Biology**

MSc, University of Louisville

2015 **Biology**

B.s. University of Louisville

Experience:

2017-present **Research Technician II**, Potempa Lab, University of
Louisville

- Proficient in all steps of protein purification process: maintenance and cultivation of bacterial cultures, collection by sonication and precipitation techniques, purification by affinity chromatography and operation of FPLC columns.
- Trained in recombinant E. coli protein purification, plasmid mutagenesis and transformation.
- Proficient in enzyme characterization methods: concentration (spectrophotometry, Nanodrop, BCA), enzyme substrate kinetics assays, enzyme inhibitor titration, gel electrophoresis, wet Western blots for immunoblotting and sequencing.
- Responsible for generation and maintenance of chemical inventories and bacterial stocks.
- Experienced with operation of most common laboratory equipment: Fume hood, Sterile hood, incubators, anaerobic chambers, gas cylinders, FPLC, sonicators, cell disruptor, spectrophotometer, pH meter, imagers.

- Proficient at growing and maintaining gingival epithelial cell lines and performing various cell experimental methodologies.
- Trained in RNA extraction from gingival epithelial cells as well as bacterial cells.
- Perform maintenance and upkeep of various lab and departmental equipment (Centrifuges, tabletop and freestanding, anaerobic chamber, -80°C freezers, incubators, sterile hoods, FPLC systems and columns, autoclave)

Publications:

Ciaston, I., Budziaszek, J., Satala, D., Potempa, B., **Fuchs, A.**, Rapala-Kozik, M., Mizgalska, D., Dobosz, E., Lamont, R. J., Potempa, J., & Koziel, J. (2022). Proteolytic Activity-Independent Activation of the Immune Response by Gingipains from *Porphyromonas gingivalis*. *mBio*, 13(3), e0378721.
<https://doi.org/10.1128/mbio.03787-21>